JOURNAL OF GEOPHYSICAL RESEARCH, VOL. 114, D22305, doi:10.1029/2009JD011900, 2009

Probing into regional O_3 and particulate matter pollution in the United States: 2. An examination of formation mechanisms through a process analysis technique and sensitivity study

Yang Zhang,[1] Xin-Yu Wen,[1] Kai Wang,[1] Krish Vijayaraghavan,[2] and Mark Z. Jacobson[3]

Received 11 February 2009; revised 31 May 2009; accepted 22 June 2009; published 25 November 2009.

[1] Following a comprehensive model evaluation in part 1, this part 2 paper describes results from 1 year process analysis and a number of sensitivity simulations using the Community Multiscale Air Quality (CMAQ) modeling system aimed to understand the formation mechanisms of O_3 and $PM_{2.5}$, their impacts on global environment, and implications for pollution control policies. Process analyses show that the most influential processes for O_3 in the planetary boundary layer (PBL) are vertical and horizontal transport, gas-phase chemistry, and dry deposition and those for $PM_{2.5}$ are primary PM emissions, horizontal transport, PM processes, and cloud processes. Exports of O_3 and O_x from the U.S. PBL to free troposphere occur primarily in summer and at a rate of 0.16 and 0.65 Gmoles day^{-1}, respectively. In contrast, export of $PM_{2.5}$ is found to occur during all seasons and at rates of 25.68–34.18 Ggrams day^{-1}, indicating a need to monitor and control $PM_{2.5}$ throughout the year. Among nine photochemical indicators examined, the most robust include $PH_2O_2/PHNO_3$, $HCHO/NO_y$, and $HCHO/NO_z$ in winter and summer, $H_2O_2/(O_3 + NO_2)$ in winter, and NO_y in summer. They indicate a VOC-limited O_3 chemistry in most areas in winter, but a NO_x-limited O_3 chemistry in most areas except for major cities in April–November, providing a rationale for nationwide NO_x emission control and integrated control of NO_x and VOCs emissions for large cities during high O_3 seasons (May–September). For sensitivity of $PM_{2.5}$ to its precursors, the adjusted gas ratio provides a more robust indicator than that without adjustment, especially for areas with insufficient sulfate neutralization in winter. NH_4NO_3 can be formed in most of the domain. Integrated control of emissions of PM precursors such as SO_2, NO_x, and NH_3 are necessary for $PM_{2.5}$ attainment. Among four types of VOCs examined, O_3 formation is primarily affected by isoprene and low molecular weight anthropogenic VOCs, and $PM_{2.5}$ formation is affected largely by terpenes and isoprene. Under future emission scenarios, surface O_3 may increase in summer; surface $PM_{2.5}$ may increase or decrease. With 0.71°C increase in future surface temperatures in summer, surface O_3 may increase in most of the domain and surface $PM_{2.5}$ may decrease in the eastern U.S. but increase in the western U.S.

Citation: Zhang, Y., X.-Y. Wen, K. Wang, K. Vijayaraghavan, and M. Z. Jacobson (2009), Probing into regional O_3 and particulate matter pollution in the United States: 2. An examination of formation mechanisms through a process analysis technique and sensitivity study, *J. Geophys. Res.*, *114*, D22305, doi:10.1029/2009JD011900.

1. Introduction

[2] Regional ozone (O_3) and fine particulate matter ($PM_{2.5}$) pollution are enhanced by many factors including emissions, in situ photochemistry, and local/synoptic meteorological processes. A number of probing techniques have been developed to provide diagnostic evaluations of three-dimensional (3-D) air quality models (AQMs) and to indicate the responses of model predictions to changes in emissions. Evaluations of several representative probing techniques such as the ozone source apportionment technology (OSAT) [*ENVIRON*, 2004], direct decoupled methods (DDM) [*Dunker*, 1984; *Milford et al.*, 1992], and process analysis (PA) [*Jang et al.*, 1995; *Tonnesen and Dennis*, 2000a, 2000b] for 3-D AQMs were conducted by *Seigneur et al.* [1999] and *Zhang et al.* [2005]. These tools permit a mechanistic examination of the chemical and physical pro-

[1]Department of Marine, Earth and Atmospheric Sciences, North Carolina State University, Raleigh, North Carolina, USA.
[2]Atmospheric and Environmental Research, Inc., San Francisco, California, USA.
[3]Department of Civil and Environmental Engineering, Stanford University, Stanford, California, USA.

0148-0227/09/2009JD011900$09.00

cesses simulated in the model and thus offer insights into the formation mechanisms and governing processes of air pollutants. PA is one such tool that enables an in-depth, quantitative understanding of various processes and their relative importance in affecting the abundance of key pollutants. PA calculates the Integrated Process Rates (IPRs) and the Integrated Reaction Rates (IRRs) for all gas-phase chemical reactions for all model grid cells. The IPRs provide the change in species concentrations due to individual atmospheric processes. The IRRs provide individual gas-phase reaction rates that can be used to determine dominant reactions and chemical regime of O_3 and its precursors [*Jeffries and Tonnesen*, 1994; *Jang et al.*, 1995].

[3] While global climate change has been shown to affect regional air quality and air pollution mortality [e.g., *Hogrefe et al.*, 2004; *Murazaki and Hess*, 2006; *Jacobson*, 2008; *S. Wu et al.*, 2008; *Heald et al.*, 2008], changes in the composition and abundance of greenhouse gases and PM can also affect air quality and climate on a global scale and in other regions downwind of sources by altering the Earth's radiation budget and background concentrations [e.g., *Jacob et al.*, 1999; *Jacobson*, 2002; *Feichter and Roeckner*, 2004; *Jacobson et al.*, 2007]. For example, NO_y and O_3 exported from the U.S. planetary boundary layer (PBL) to the free troposphere will affect global O_3 pollution [e.g., *Jacob et al.*, 1993; *Liang et al.*, 1998; *Horowitz et al.*, 1998; *Li et al.*, 2004; *Pierce et al.*, 2007; *Vijayaraghavan et al.*, 2009]. The long-range transport of gases and aerosols from Asia to the U.S. also has potentially important impacts on air quality control in the U.S. [e.g., *Jacob et al.*, 1999; *Wang et al.*, 2009].

[4] In this study, a 1 year baseline simulation for 2001 over continental U.S. (CONUS), southern Canada, and northern Mexico has been conducted using the Pennsylvania State University (PSU)/National Center for Atmospheric Research (NCAR) Mesoscale Modeling System Generation 5 (MM5) version 3.6.1 and the Community Multiscale Air Quality (CMAQ) Modeling System version 4.4 [*Byun and Schere*, 2006]. The results were evaluated with available surface and satellite observations in part 1 [*Zhang et al.*, 2009]. The evaluation shows an overall satisfactory performance for annual mean maximum 1 h and 8 h average O_3 mixing ratios, 24 h average concentrations of $PM_{2.5}$, wet deposition fluxes, and column abundance of CO and NO_2. In this paper, the relative importance of major atmospheric processes in governing the fate of key pollutants is examined and the total mass exported from the U.S. PBL to the global atmosphere is estimated using IPRs from the CMAQ-PA tool. The sensitivity of O_3 and $PM_{2.5}$ formation to their precursor emissions is studied using the IRRs products and additional indicators to support emission control policies. In addition, a number of sensitivity simulations are conducted to study the effect of emissions and model treatments on O_3 and $PM_{2.5}$ and potential impacts on the global environment under both current and future emission scenarios.

2. Process Analysis Approach and Sensitivity Simulation Design

[5] The process analysis is conducted using the PA tool imbedded in CMAQ from the same CMAQ baseline simulation described by *Zhang et al.* [2009]. Hourly IPRs for 30 species and IRRs for 96 gas-phase reactions in the Carbon Bond Mechanism (CBM)-IV are calculated. The hourly IPRs are analyzed for key pollutants for surface layer and layers 1–10 in the PBL (corresponds to surface to ~2.9 km above ground level (AGL)) to examine the relative importance of major atmospheric processes such as emissions of primary species, horizontal transport (including advection and diffusion), vertical transport (including advection and diffusion), gas-phase chemistry (including photolysis and kinetic reactions), dry deposition, cloud processes (including cloud attenuation of photolytic rates, convective and nonconvective mixing and scavenging by clouds, aqueous-phase chemistry, and wet deposition), and PM microphysical processes (including thermodynamic equilibrium of inorganic and organic species and dynamics such as homogeneous nucleation, condensation/evaporation, and coagulation, referred to PM processes hereafter for simplicity). Major species of interest include sulfur dioxide (SO_2), nitrogen oxides (NO_x = nitric oxide (NO) + nitrogen dioxide (NO_2)), total reactive nitrogen (NO_y = NO_x + nitrogen trioxide (NO_3) + dinitrogen pentoxide (N_2O_5) + nitrous acid (HONO) + nitric acid (HNO_3) + pernitric acid (HNO_4) + peroxyacyl nitrate (PAN)), O_3, total odd oxygen (O_x = O_3 + NO_2 + 2 × NO_3 + oxygen atom (O) + excited state oxygen atom (O^1D) + PAN + 3 × N_2O_5 + HNO_3 + HNO_4 + unknown organic nitrate), anthropogenic and biogenic volatile organic compounds (AVOCs and BVOCs), and $PM_{2.5}$ and its major components such as ammonium (NH_4^+), sulfate (SO_4^{2-}), nitrate (NO_3^-), organic matter (OM), black carbon (BC), and other inorganic aerosols (OIN). Total exports of each of these pollutants from the PBL are calculated as the sum of process contributions of emissions, gas-phase chemistry, PM processes, cloud processes, and dry deposition in the PBL. The positive values indicate export out of the PBL into the free troposphere, and the negative values indicate import from the free troposphere into the PBL.

[6] Table 1 lists 34 IRRs products that offer insights into the gas-phase chemistry and indicate whether O_3 formation is NO_x- or VOC-limited. For example, the net production and loss of O_x, Total OxProd and Total OxLoss, respectively, represent the total oxidation capacity that affects the formation efficiency of O_3 and secondary PM. The hydroxyl radical (OH) chain length, OH_CL, is the average number of times a newly created OH radical will be recreated through radical chain propagation before it can be removed from the cycle [*Seinfeld and Pandis*, 2006]. It provides a measure of relative importance of O_3-forming reactions versus radical terminations or other non-O_3 forming reactions, and therefore an overall efficiency of a gas-phase chemical mechanism in converting NO to NO_2 for O_3 formation in the atmosphere. The production of HNO_3 can be calculated as the sum of HNO_3 produced from three reactions: OH with NO_2 (HNO_3_$OHNO_2$), hydrocarbons (HC) with NO_3 (HNO_3_NO_3HC), and N_2O_5 with water (HNO_3_N_2O_5)). The ratio of production rate of hydrogen peroxide (H_2O_2) (H_2O_2Prod) to production rate of HNO_3, P_{H2O2}/P_{HNO3}, can determine NO_x- or VOC-limited O_3 chemistry [*Sillman*, 1995; *Sillman et al.*, 1997; *Tonnesen and Dennis*, 2000a]. Detailed analyses for IPRs and IRRs are conducted domain-wide and at 16 locations representative of air masses with different emissions/meteorological characteristics in different regions of the continental U.S.

Table 1. IRRs Outputs for the CBM-IV From CMAQ-PA

Product Type	Product Name	Chemical Representation
Ox budget	Total O_xProd	O_x chemical production
	Total O_xLoss	O_x chemical destruction
Radical initiation	newOH_O^1D	New OH from O^1D+H_2O
	newOHother	New OH from H_2O_2, HNO_3, HONO, PAA, OP1, OP2, O_3 + HC (except isoprene)
	newHO_2_HCHO	New HO_2 from HCHO
	newHO_2tot	New HO_2 production (total)
	newRO_2tot	New RO_2 production (total)
	nHO_x_isop	New HO_x (including OH, HO_2, and RO_2) from isoprene
Radical propagation	OHwCO_CH_4	Sum of OH+CO and OH+CH_4 reactions
	ISOPwOH	OH+ISOP
	ISOPwO_x	Isoprene reactions with O_3, NO_3, and O^3P
	OH_VOC	OH reacted with anthropogenic VOC
	OHw_all_HC	OH reacted with all VOCs including isoprene
	OHpropmisc	Other OH propagation reactions (e.g., OH+SO_2)
	HO_2TotProd	Total HO_2 production
	RO_2TotProd	Total RO_2 production
	HO_2_to_NO_2	NO_2 produced from reactions of HO_2
	HO_2_to_OH	OH produced from reactions of HO_2
	RO_2_to_NO_2	NO_2 produced from reactions of RO_2
	OH_reacted	Total OH production
Radical termination	OHterm	OH termination
	HO_2term	HO_2 termination
	RO_2term	RO_2 termination
	H_2O_2Prod	Production of H_2O_2
Formaldehyde production	HCHOp_isop	HCHO produced from isoprene reactions
	HCHOp_Tot	HCHO produced from all reactions
NO_x termination	HNO_3_$OHNO_2$	OH + NO_2 → HNO_3
	HNO_3_NO_3HC	NO_3 + HC → HNO_3
	HNO_3_N_2O_5	N_2O_5 + H_2O → 2 HNO_3
	HNO_3reacted	HNO_3 reacted (to produce NO_x)
	PANprodNet	Net PAN production
	PANlossNet	Net PAN loss (source of NO_x and a radical)
	RNO_3_prod	Production of organic nitrates
Overall oxidation efficiency	OH_CL	OH chain length

(CONUS) (e.g., urban versus rural, inland versus coast, NO_x-limited versus VOC-limited) (see site locations in Figure 1 of *Zhang et al.* [2009]). The 16 sites include 2 from the Southeastern Aerosol Research and Characterization study (SEARCH) (i.e., Jefferson Street (JST), Atlanta, GA; Yorkville (YRK), GA); 12 from the Aerometric Information Retrieval System−Air Quality System (AIRS-AQS) (i.e., Big Bend NP (BBE), TX, Great Smoky National Park (GRS), TN; Olympic National Park (OLY), WA; Yellowstone National Park (YEL), WY; Chicago (CHI), IL; Fresno (FRE), CA; Houston (HOU), TX; Los Angeles (LAX), CA; New York city (NYC), NY; Pittsburgh (PIT), PA; Riverside (RIV), CA; Tampa (TAM), FL), 5 from the Clean Air Status and Trends Network (CASTNET) (i.e., BBE, GRS; OLY; YEL; and Penn State University (PSU), PA), and 4 from the Interagency Monitoring of Protected Visual Environments (IMPROVE) (i.e., BBE, GRS, YEL, and Grand Canyon National Park (GRC), AZ) (note that 7 of the above sites belong to multiple networks). While the use of a 36 km horizontal grid resolution is representative for large city sites such as HOU, CHI, NYC, and LAX, it may be too coarse to accurately represent dominant processes and total budget of chemical species for small city/rural/national park sites that are smaller than the grid size of 36 × 36 km^2.

[7] In addition to P_{H2O2}/P_{HNO3} calculated based on the IRRs outputs, several photochemical indicators including H_2O_2/HNO_3, $H_2O_2/(O_3 + NO_2)$, NO_y, O_3/NO_x, O_3/NO_y, O_3/NO_z (where $NO_z = NO_y - NO_x$), formaldehyde (HCHO)/NO_y, and HCHO/NO_2 are used to provide a better understanding of O_3 chemistry. Table 2 summarizes these indicators along with the transition values based on the literature as well as those recommended by this study (in parentheses) to indicate NO_x- and VOC-limited O_3 chemistry. Compared with photochemical indicators, indicators for the sensitivity of $PM_{2.5}$ formation to its precursor emissions/concentrations have been reported in fewer studies, because of complexity in its dependence on gas-phase mechanism, aerosol thermodynamics, and meteorological conditions such as temperature (T) and relative humidity (RH) [e.g., *Ansari and Pandis*, 1998; *Takahama et al.*, 2004; *S.-Y. Wu et al.*, 2008; *Pinder et al.*, 2008]. Table 3 lists three indicators along with their transition values used in this study for the PM sensitivity: the degree of sulfate neutralization (DSN), gas ratio (GR), and adjusted gas ratio (AdjGR). The theoretical basis for photochemical indicators is given by *Stockwell* [1986], *Milford et al.* [1994], *Sillman* [1995], and *Tonnesen and Dennis* [2000a, 2000b] and those for PM sensitivity indicators are given by *Ansari and*

Table 2. Photochemical Indicators and Threshold Values Used for NO_x- or VOC-Sensitivity of O_3 Chemistry in This Study

Indicators	NO_x-Limited (ppb)	VOC-Limited (ppb)	References
P_{H2O2}/P_{HNO3}	$\geq$0.2[a]	<0.2[a]	*Sillman* [1995], *Tonnesen and Dennis* [2000a]
H_2O_2/HNO_3	$\geq$0.2 (2.4)[b,c]	<0.2 (2.4)[c]	*Sillman* [1995], *Sillman et al.* [1997], *Lu and Chang* [1998], *Tonnesen and Dennis* [2000b], *Hammer et al.* [2002], *Liang et al.* [2006]
$H_2O_2/(O_3 + NO_2)$	$\geq$0.02 (0.04 for summer)[c]	<0.02 (0.04 for summer)[c]	*Tonnesen and Dennis* [2000b]
NO_y	$\leq$20 (5)[c,d]	>20 (5)[c,d]	*Milford et al.* [1994], *Sillman* [1995], *Lu and Chang* [1998], *Vogel et al.* [1999]
O_3/NO_x	$\geq$15 (60)[c,e]	<15 (60)[c,e]	*Tonnesen and Dennis* [2000a, 2000b], *Liang et al.* [2006]
O_3/NO_y	$\geq$7 (15)[c,f]	<7 (15)[c,f]	*Sillman et al.* [1997], *Liang et al.* [2006]
O_3/NO_z	$\geq$7 (100 for winter, 20 for summer)[c,g]	<7 (100 for winter, 20 for summer)[c,g]	*Sillman* [1995], *Lu and Chang* [1998], *Liang et al.* [2006]
$HCHO/NO_y$	$\geq$0.28[h]	<0.28	*Sillman* [1995], *Lu and Chang* [1998]
$HCHO/NO_2$	$\geq$1	<1	*Tonnesen and Dennis* [2000b], *Martin et al.* [2004]

[a]A transition value of 0.5 for $P_{total\ peroxides}/P_{HNO3}$ was proposed by *Sillman* [1995], where total peroxides = H_2O_2 + organic peroxides (ROOH). *Tonnesen and Dennis* [2000a, 2000b] reported transition values of P_{H2O2}/P_{HNO3} of <0.06, 0.06–0.2, and >0.2, corresponding to VOC-limited, ridgeline, and NO_x-limited conditions, respectively.

[b]A transition value proposed was 0.4 by *Sillman* [1995], 0.2 by *Sillman et al.* [1997], 0.8–1.2 by *Lu and Chang* [1998], and 0.2 by *Tonnesen and Dennis* [2000b] and *Hammer et al.* [2002]. *Liang et al.* [2006] reported a range of transition values of 0.34–3.6 for total peroxides/HNO_3 under summer conditions over CA.

[c]Transition values recommended in this study based on analyses of results.

[d]A transition value proposed was 10–25 ppb by *Milford et al.* [1994], 20 ppb by *Sillman* [1995], and 3–5 ppb by *Lu and Chang* [1998]. *Vogel et al.* [1999] [1999] reported a transition value of 7.78 ppb based on observations and 26–30 ppb based on box model studies but noted that the transition value varies with emissions, temperature, relative humidity, and radiation and no universal transition values were found.

[e]A transition value proposed was 15 by *Tonnesen and Dennis* [2000a] and 6.8 to >400 by *Liang et al.* [2006], where >400 indicates an open range for an upper bound.

[f]A transition value proposed was 7 by *Sillman et al.* [1997] and 5.1–40 by *Lu and Chang* [1998].

[g]A transition value proposed was 7 by *Sillman* [1995], 25–30 by *Lu and Chang* [1998], and 12–48 by *Liang et al.* [2006].

[h]A transition value proposed was 0.28 by *Sillman* [1995] and 0.5–0.9 by *Lu and Chang* [1998].

Table 3. Indicators for Sensitivity of $PM_{2.5}$ Formation to Precursor Concentrations[a]

Indicators	Transition Values	Meaning	References
Degree of sulfate neutralization (DSN)	$\geq$2 (1.5)[b]	SO_4^{2-} is fully neutralized; potential NH_4NO_3 formation if free NH_3 is available	*Pinder et al.* [2008]
	<2 (1.5)[b]	SO_4^{2-} is insufficiently neutralized; no NH_4NO_3 formation	
Gas ratio (GR)[c]	<0	NH_3^- poor condition; insufficient NH_3 to neutralize SO_4^{2-}; no NH_4NO_3 formation; PM formation is insensitive to an increase in TS; nonlinear enhanced increase to an increase in TA; and insensitive to an increase in TN; PM nitrate concentration is most sensitive to changes in NH_3 because of abundance of TN;	*Ansari and Pandis* [1998], *Takahama et al.* [2004], *S.-Y. Wu et al.* [2008]
	0–1	NH_3^- nuetral condition; sufficient NH_3 to neutralize SO_4^{2-}; no NH_4NO_3 formation; PM response to an increase in TS ranges from nonlinear enhanced increase to insensitive at $T \leq 298$ K depending on RH and TN; PM response to an increase in NH3 ranges from insensitive to nonlinear near-constant increase depending on T, RH, and TN; PM response to an increase in TN ranges from insensitive to nonlinear enhanced increase depending on T, RH, and TA; PM nitrate concentration is most sensitive to changes in NH_3 because of abundance of TN	
	>1	NH_3^- rich condition; sufficient NH_3 to neutralize SO_4^{2-} and NO_3^-; potential NH_4NO_3 formation; PM response to an increase in TS is generally nonlinear enhanced increase at $T \leq 275$ K and linear constant increase at $T > 275$ K; PM response to an increase in NH3 ranges from nonlinear enhanced increase to insensitive depending on T, RH, and TN; PM response to an increase in TN ranges from insensitive to linear reduced increase depending on T, RH, and TA; PM nitrate concentration is most sensitive to changes in TN because of abundance of free NH_3	
Adjusted Gas Ratio (AdjGR)[c]	The same as above	The same as above, but more robust under insufficient sulfate neutralization condition than GR. While GR is defined with an assumption of full sulfate neutralization, i.e., concentration of free NH_3 = [TA] − 2 × [TS], AdjGR does not require this assumption, concentration of free NH_3 = [TA] − DSN × [TS]	*Pinder et al.* [2008], *S.-Y. Wu et al.* [2008]

[a][TA] is the total molar concentration of NH_3, = [NH_3] + [NH_4^+]; [TS] is the total molar concentration of SO_4^{2-}, = [SO_4^{2-}], [TN] is the total molar concentration of NO_3^-, = [NO_3^-] + [HNO_3]; concentration of free NH_3 = [TA] − 2 × [TS] for GR but = [TA] − DSN × [TS] for AdjGR.

[b]A transition value recommended in this study based on analyses of results.

[c]The transition values for GR or AdjGR vary with ambient temperature (T), relative humidity (RH), and chemical conditions. While the values of 0, 0–1, and 1 provide an accurate representation of the chemical regime transition based on neutralization theory for the NH_3-H_2SO_4-HNO_3-H_2O system, they may be somewhat different for other systems or under various combinations of meteorological and chemical conditions as described by *Ansari and Pandis* [1998].

Table 4. Sensitivity Simulations Conducted in This Study

Simulation Index	Time Period	Differences From the Baseline Simulation
C1	Jan. and Aug. 2001	Same as baseline simulation but without isoprene emissions
C2	Jan. and Aug. 2001	Same as baseline simulation but without terpene emissions
C3	Jan. and Aug. 2001	Same as baseline simulation but without low molecular weight (MW) anthropogenic VOC emissions (i.e., HCHO, ALD2, PAR, OLE, and ETH)
C4	Jan. and Aug. 2001	Same as baseline simulation but without high MW anthropogenic VOC emissions (i.e., TOL and XYL)
C5	Jan. and Aug. 2001	Same as baseline simulation but with isoprene SOA formation
C6	Jan. and Aug. 2001	Same as baseline simulation but cloud processes including aqueous-phase chemistry, cloud scavenging, and wet deposition) are turned off
F1[a]	Jan. and Aug. 2001	Same as baseline simulation but with projected emissions for 2020 by IPCC SRES A1B scenario, with significant increases in the total global emissions of NO_x (by 44.06%), VOCs (by 57.45%), and SO_2 (by 45.22%) and moderate increases in those of CO (by 17.67%), BC (by 15.32%) and OM (by 14.99%).
F2[a]	Jan. and Aug. 2001	Same as baseline simulation but with projected emissions for 2020 by IPCC SRES B1 scenario, with moderate increases in the total global emissions of NO_x (by 24.69%) and SO_2 (by 8.12%) but small-to-moderate decreases in those of CO (by −14.37%), VOCs (by −0.71%), BC (by −12.1%), and OM (by −12.16%).
F3[a]	Jan. and Aug. 2001	Same as baseline simulation but with projected emissions for 2020 by IPCC SRES B2 scenario, with moderate increases (8–25%) in the total global emissions of NO_x (by 33.44%), CO (by 16.53%), VOCs (by 27.66%), BC (13.71%), and OM (14.0%) and but moderate decreases in those of SO_2 (by −11.16%).
F4[b]	Aug. 2001[c]	Same as baseline simulation but with increased emissions of biogenic species (e.g., isoprene, terpenes, and NO_2), generated with the biogenic emissions inventory System (BEIS version 3.12) and SMOKE emission processor by increasing PBL temperatures by 0.71°C.

[a]The 2020 emissions of CO, NO_x, VOCs, SO_2, BC, and OM are scaled from the baseline emissions with the scaling factors from IPCC SRES emission scenarios [*IPCC*, 2001].
[b]An increase of temperature of 0.71°C is the largest temperature change projected by IPCC for 2020 among all SRES future scenarios [*IPCC*, 2001].
[c]F4 simulation is conducted for August only because the emissions of BVOCs are much higher in summer and also respond much stronger to changes in temperatures in summer.

Pandis [1998], *Nguyen and Dabdub* [2002], *Takahama et al.* [2004], and *Pinder et al.* [2008]. *Andreani-Aksoyoglu et al.* [2001] studied the robustness of some of the photochemical indicators under various meteorological and chemical conditions and found that their transition values vary strongly with ambient conditions and locations. *Liang et al.* [2006] evaluated several indicators such as O_3/NO_x, O_3/NO_y, O_3/NO_z, $HCHO/NO_y$, and total peroxides ($HO_2 + RO_2$)/HNO_3 and found that these indicators have a wide range of transition values that exhibit strong spatial variability, which makes it difficult to determine unambiguously precursor limitations of maximum 8 h O_3. In light of self-inconsistency of some indicators and large uncertainties associated with the transition values, *Zhang et al.* [2009] recommended the use of a set of indicators (rather than a single indicator) for a complete assessment of O_3.

[8] The model setup for the 1 year baseline simulation is described by *Zhang et al.* [2009]. A set of sensitivity experiments are conducted for two 1 month periods: January and August under both current (i.e., 2001) and future (i.e., 2020) climate and emission conditions, as summarized in Table 4. The current-year simulations C1–C4 are designed to show the relative importance of isoprene, terpenes, and low and high molecular weight (LMW and HMW) AVOCs (i.e., with the number of carbons <8 and ≥8, respectively) to O_3 and $PM_{2.5}$ formation. While zeroing out emissions of each of the four VOC categories is not practical from the emission control perspective because biogenic emissions are not controllable and anthropogenic emissions cannot be 100% removed, understanding of their roles in O_3 and $PM_{2.5}$ formation via such sensitivity studies will provide information valuable for the development of emission control strategies. Since CMAQ v4.4 does not treat SOA formation from isoprene photo-oxidation, C5 is conducted to estimate the importance of isoprene SOA formation using the modified SOA module of *Zhang et al.* [2007]. C6 is designed to examine the effect of cloud processes on the formation of O_3 and $PM_{2.5}$. The future-year simulations F1–F3 are conducted under the Intergovernmental Panel on Climate Change projected Special Report on Emissions Scenarios (SRES) A1B, B1, and B2 for year 2020 [*Intergovernmental Panel on Climate Change* (*IPCC*), 2001], respectively; they provide the responses of simulated O_3 and $PM_{2.5}$ to future emission changes. In F1–F3, 2020 emissions of carbon monoxide (CO), NO_x, VOCs, SO_2, BC, and OM are scaled from the baseline emissions with the scaling factors from *IPCC* [2001]. F4 is aimed to examine the effect of increased emissions of BVOCs (e.g., isoprene and terpene) as a result of the largest temperature increase (by 0.71°C) projected for the 2020 IPCC SRES scenario on O_3 and $PM_{2.5}$. Since the emissions of BVOCs are much higher in summer and also respond much more to changes in temperatures than in winter, F4 is conducted for August only.

3. Analyses of Integrated Process Rates (IPRs)

3.1. Controlling Processes for Chemical Species at Surface

[9] Figure 1 shows the monthly mean hourly contributions of atmospheric processes to changes in surface maximum 8 h O_3 at the 16 sites. Vertical transport is the predominant process at all sites for the accumulation of maximum 8 h O_3, which may be formed upwind and transported to the 16 sites via horizontal and/or vertical transport. Local gas-phase chemistry contributes to maximum 8 h O_3 production by up to 14 ppb h^{-1} at rural sites (i.e., YRK and PSU) and urban/suburban sites (i.e., LAX, FRE, RIV, JST, TAM, and PIT) starting as early as February

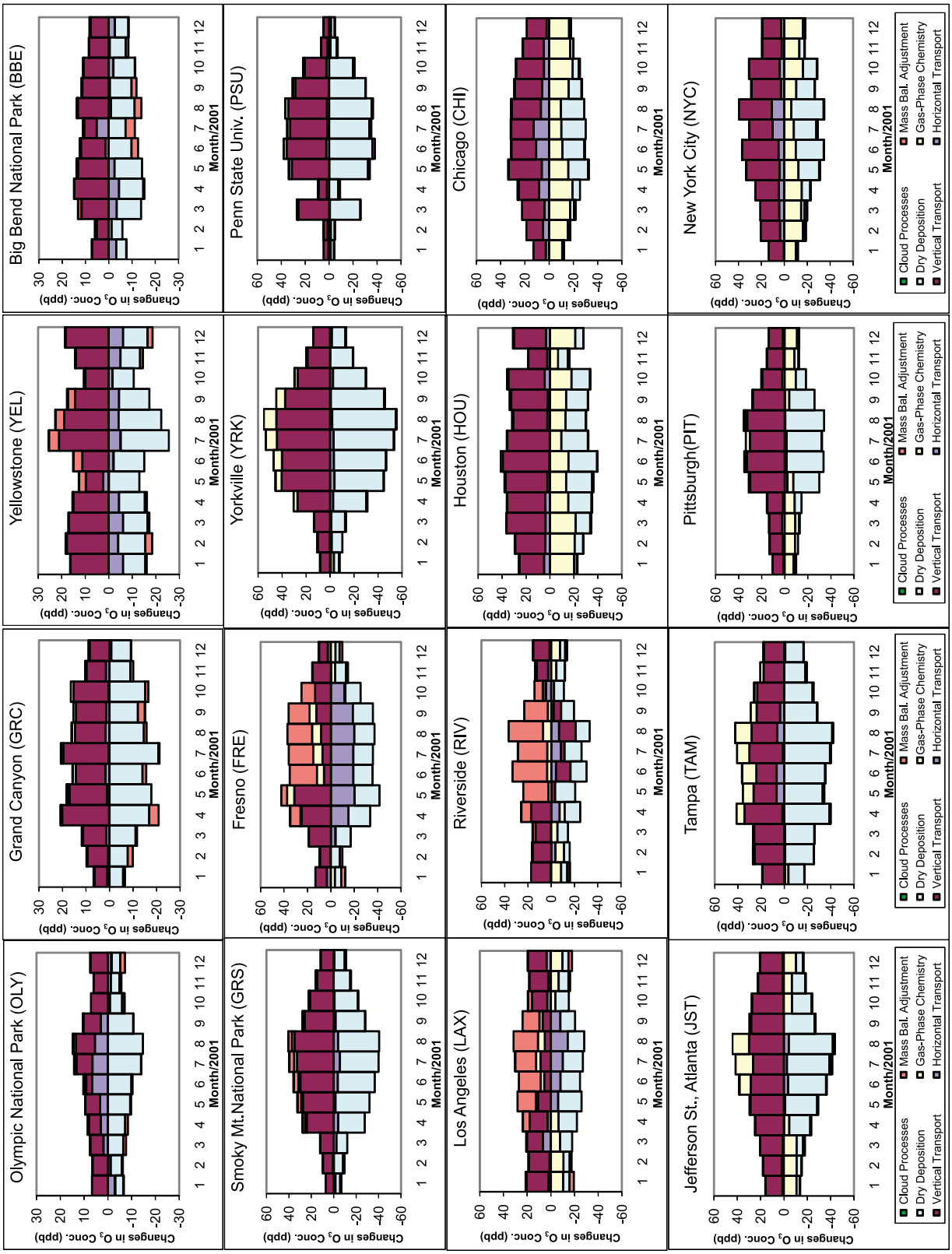

Figure 1. Monthly mean hourly contributions of individual processes to the surface mixing ratios of maximum 8 h O_3 at 16 sites over CONUS in 2001.

and ending as late as December and by up to 2.7 ppb h^{-1} at national park sites (i.e., OLY, GRC, YEL, BBE, and GRS) during most months. It, however, contributes to maximum 8 h O_3 destruction by up to 21.4 ppb h^{-1} in three large cities (i.e., HOU, CHI, and NYC) throughout the year and in other cities (e.g., LAX, RIV, TAM, and PIT) during some months, due to the dominance of NO titration at those sites in the presence of large NO sources. Dry deposition is the predominant removal process for maximum 8 h O_3 at all sites, although horizontal transport sometimes carries it out of some sites (e.g., YEL, BBE, GRS, LAX, and RIV) and gas-phase chemistry destroys it in the aforementioned cities. Cloud processes such as convective mixing, aqueous-phase chemistry, cloud scavenging, and wet deposition make negligible contributions to maximum 8 h O_3 at all sites, although they may be important to domain-wide O_x budget (see Figure 4). Large mass balance adjustment occurs at all sites during summer in CA (i.e., LAX, FRE, and RIV) because of a complex terrain in this region that causes numerical difficulties in solving advection and chemistry in the model, and the rates of changes in O_3 and differences in the lifetimes of species are generally greater in summer than in winter. Such an adjustment is no longer needed in CMAQ v4.5 or newer because of the use of an advanced advection scheme. The differences in process contributions at different sites reflect differences in meteorological conditions, emissions, and geographic characteristics at these sites. For example, located downwind of major sources of Ohio Valley, NYC is positively affected by horizontal transport; this is in contrast with JST and YRK where local chemistry plays an important role in O_3 accumulation. This implies that emission control efforts should focus on local sources for JST and YRK but consider both local and upwind sources for NYC. FRE and LAX are largely affected by horizontal transport which blows air pollutants from source areas into inland areas, indicating the role of sea breezes/surface winds in cleansing the atmosphere at those sites. An examination of diurnal changes in O_3 mixing ratios at each site can provide further insights into the roles of atmospheric processes (figure not shown). For example, on June 6, gas-phase chemistry produces up to 10.5 ppb h^{-1} of O_3 between noon and 5 P.M., eastern standard time (EST) at TAM and 24.7 ppb h^{-1} of O_3 between 10 A.M. and 3 P.M., PST at LAX. Horizontal transport increases O_3 during morning hours at LAX because the transport of hot, polluted airs from inland areas where T is higher than LAX and tends to increase O_3, whereas the afternoon winds and sea breeze help cleanse the air (i.e., reducing O_3 level) as they transport O_3 and its precursors such as NO_x emitted at LAX eastward out of the Los Angeles basin.

[10] Figure 2 shows the monthly mean contributions of individual processes to the changes in the surface concentrations of $PM_{2.5}$ at the 16 sites. Primary PM emissions are the predominant contributor to $PM_{2.5}$ production at all sites except for two national park sites (i.e., YEL and GRS) where vertical transport dominates. Horizontal transport also helps accumulate $PM_{2.5}$ at two suburban/rural sites (i.e., FRE and PSU) during some months. PM processes (e.g., gas-to-particle conversion processes such as chemical equilibrium, absorption, and condensation, and growth processes such as coagulation) produce $PM_{2.5}$ by increasing the levels of secondary PM such as NO_3^-, NH_4^+, and secondary organic aerosol (SOA) at all sites except 5 (i.e., LAX, FRE, RIV, GRC, and YEL), with higher accumulation rates occurring in large cities such as NYC, JST, PIT, HOU, TAM, and CHI (by up to 4.5, 3.4, 3.3, 2.6, 2.4, and 1.9 $\mu g\ m^{-3}\ h^{-1}$, respectively) and at rural/suburban sites such as YRK, PSU, and RIV (by up to 2.2, 1.8, and 1.0 $\mu g\ m^{-3}\ h^{-1}$, respectively). Some PM processes (e.g., evaporation and desorption) remove $PM_{2.5}$ by up to 0.07, 0.8, and 2.13 $\mu g\ m^{-3}\ h^{-1}$ at LAX, FRE, and RIV, respectively, during dry seasons (e.g., April–October), by up to 0.09 and 0.43 $\mu g\ m^{-3}\ h^{-1}$ at GRC and YEL, respectively, during most months, and by 0.02 $\mu g\ m^{-3}\ h^{-1}$at GRS in May. This is because of the high T and low RH conditions that do not favor gas-to-particle conversions at those sites in those months. Vertical transport contributes predominantly to $PM_{2.5}$ loss via mixing and ventilation processes at most sites throughout the year. Other contributors to $PM_{2.5}$ loss include horizontal transport (e.g., CHI, RIV, JST, and HOU in all months and YRK and LAX in some months), cloud processes (e.g., HOU, CHI, JST, NYC, YRK, and PSU in all months and LAX and FRE in wet seasons (e.g., November, December, January–March) in CA, and dry deposition (e.g., NYC, YRK, PSU, and GRS). By design, the PA tool accounts for the contribution of gas-phase chemistry as part of that of PM processes, rather than as a direct contribution to $PM_{2.5}$ formation.

[11] While the fate of primary PM species such as BC, primary OM, and OIN is governed by emissions and transport, that of secondary PM is more intricate. As shown in Figure 3, PM processes dominate the accumulation of NO_3^- for all months at CHI, JST, and NYC but only in January–February at LAX, indicating a dominance of the gas-to-particle conversion processes (e.g., condensation and dissolution of HNO_3 onto the surface of PM). Vertical transport contributes to NO_3^- accumulation in all months except for August at LAX. It is a major contributor to NO_3^- loss during most months at other sites. Cloud processes (e.g., scavenging and wet deposition) provide an important removal pathway for NO_3^- during a few months at the four sites. PM processes either dominate the SOA accumulation (e.g., at JST in all months) or its depletion (e.g., at CHI and NYC in most months), indicating a competition between PM production (e.g., condensation and absorption) and destruction processes (e.g., evaporation and desorption). SOA production is much higher at JST because of the abundance of BVOCs in the southeastern U.S. which contribute to most SOA formation [*Zhang et al.*, 2007]. Vertical transport is the predominant process for SOA production at CHI and NYC, and horizontal transport of SOA and its gaseous precursors from upwind locations also plays an important role at NYC. Their contributions can be either ways at LAX, depending on the net effects of large scale transport and local winds. Dry deposition is an important removal process at NYC, CHI, and LAX because of a dominance of hydrophobic SOA produced from BVOCs that cannot effectively dissolve in cloud droplets and be removed by wet scavenging, whereas vertical transport, cloud processes, and dry deposition are important removal processes at JST. The controlling processes for NO_3^- and SOA at LAX exhibit a strong monthly variation, indicating a complex interplay among emissions, PM processes, and meteorology over complex terrains.

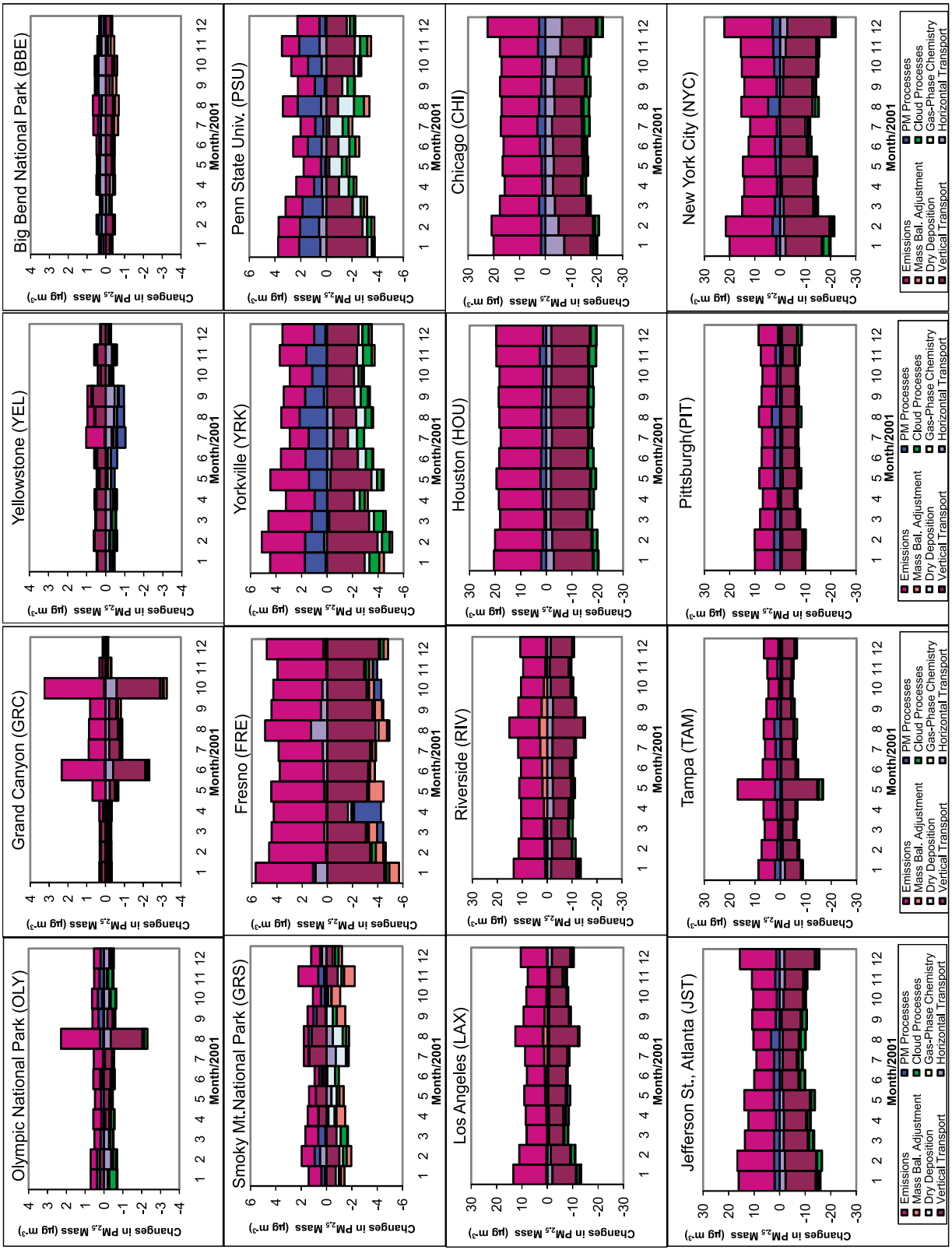

Figure 2. Monthly mean hourly contributions of individual processes to the mass concentrations of $PM_{2.5}$ at 16 sites over CONUS in 2001.

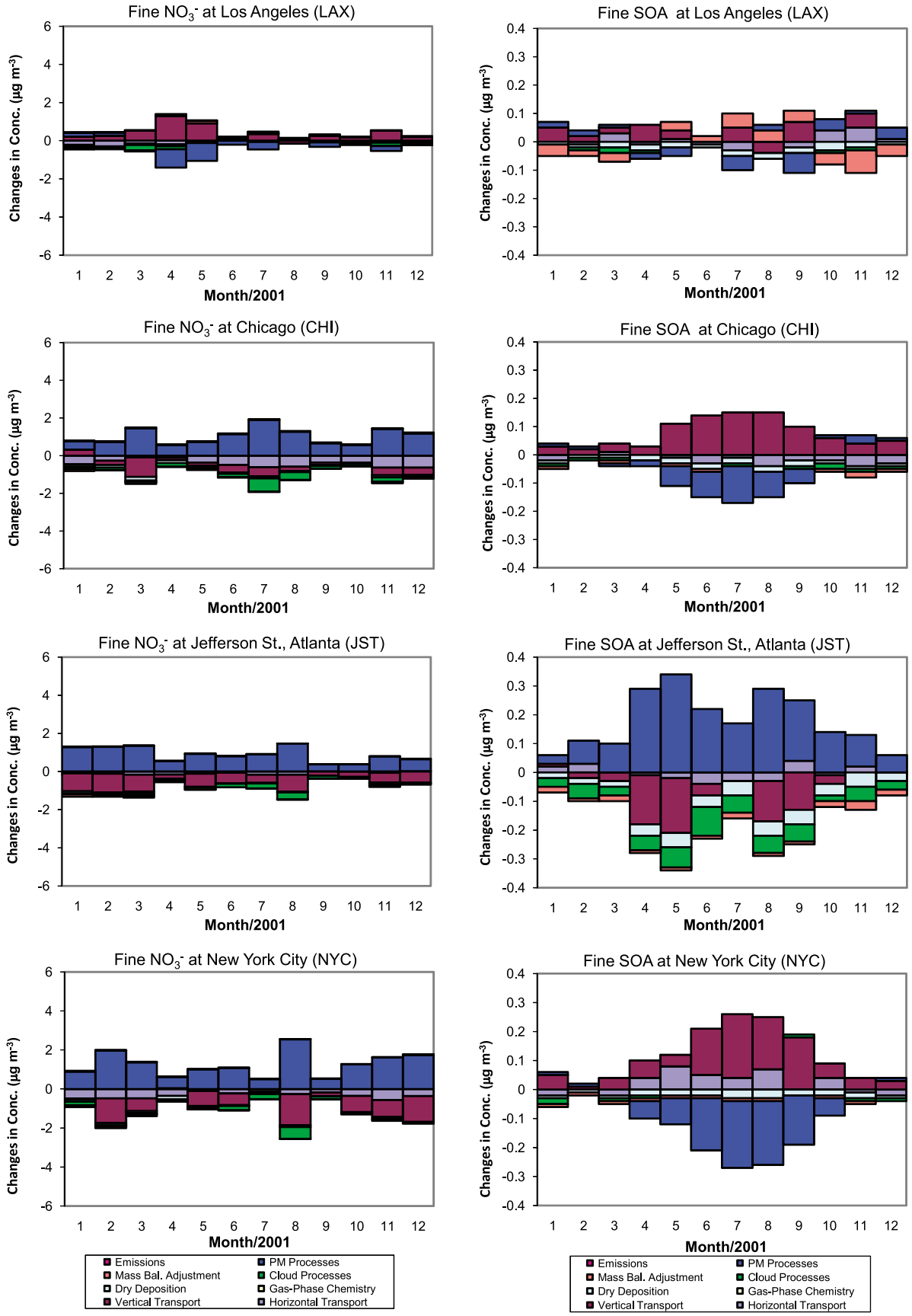

Figure 3. Monthly mean contributions of individual processes to the changes in the mass concentrations of (left) fine nitrate and (right) secondary organic aerosols (SOA) at Los Angeles (LAX), Chicago (CHI), Jefferson Street, Atlanta (JST), and New York City (NYC) in 2001.

3.2. Controlling Processing in the PBL and Exports From the PBL to Global Environment

[12] Figure 4 shows the controlling processes for O_x, NO_y, fine nitrate (NO_3^-), and $PM_{2.5}$ in the PBL for the entire domain in winter (December, January, and February (DJF)), spring (March, April, and May (MAM)), summer (June, July, and August (JJA)), and fall (September, October, November (SON)). The process contributions to O_3 formation are very similar to those of O_x formation (figure not shown), as O_3 contributes the most to O_x among all O_x species. Vertical transport and gas-phase chemistry dominate the O_x accumulation throughout all seasons and cloud processes are also an important contributor to O_x accumulation in all seasons except for winter. While cloud scavenging, aqueous-phase chemistry, and wet deposition provide direct removal processes for all gases such as O_3, NO_x, NO_y, SO_2, OH, HO_2, H_2O_2, AVOCs, and BVOCs, the vertically convective cloud transports high O_3 from the free troposphere to the PBL, leading to a net increase in domain-wide O_3 (thus O_x) mixing ratios in the PBL with a maximum occurring in summer and a minimum occurring in winter. For O_x depletion, dry deposition and horizontal transport dominate throughout the year. The contribution of NO_2 emissions to O_x accumulation and that of PM processes to O_x depletion are relatively small. The relative importance of all processes is similar in winter, spring, and fall, but somewhat different in summer during which gas-phase chemistry and convective transport of clouds from the free troposphere dominate over vertical transport for O_x accumulation and the contribution of dry deposition to O_x depletion is much greater than that of horizontal transport. Emissions of NO_x dominate the production of NO_y, all other processes contribute to NO_y depletion, with dry deposition, cloud processes, and transport as the top three contributors and little seasonal variations for their roles. The formation of NO_3^- requires cold T and sufficiently high concentrations of precursors such as HNO_3. PM processes are a dominant contributor to NO_3^- production in winter, spring, and fall, with the maximum occurring in spring during which the precursor emissions/concentrations are sufficiently large and T is not too high; both favor its formation. During summer, although precursor emissions are the highest among all seasons, the high T prevents HNO_3 from condensing onto the existing PM surface to form NO_3^-, resulting in a dominance of evaporation and desorption for total nitrate formation thus a negative contribution from PM processes. Cloud processes dominate the removal of NO_3^- in all seasons, with a maximum in spring. Horizontal and vertical transport also contribute to the removal of NO_3^- in all seasons except in summer vertical transport increases NO_3^- via a strong mixing that could have brought NO_3^- formed in upper layers (where cold temperatures favor its formation) down to the PBL. Compared to O_x and NO_y, domain-wide NO_3^- formation shows a strong seasonality, with a maximum production in spring and a minimum production in summer. The important processes for $PM_{2.5}$ production in PBL in all seasons include PM processes and primary emissions. Their nearly equal contributions for spring, summer, and fall indicate the importance of controlling both primary PM emissions and gaseous precursors of secondary PM formation. Controlling primary PM emissions may be more effective than those of gas precursor emissions in winter. Cloud processes and horizontal/vertical transport dominate its removal in all months. Unlike O_x and O_3, PM levels are higher near surface than in the upper layer; therefore, mass losses due to cloud convective mixing contribute to its losses (rather than its gain). The negative impacts of convective mixing and other cloud processes such as scavenging and wet deposition dominate over the aqueous-phase production of SO_4^{2-}, resulting in a net domain-wide loss in $PM_{2.5}$ due to cloud processes in all seasons.

[13] Table 5 gives the net exports of major pollutants from the U.S. PBL. The net exports for O_x and O_3 are -1.18 and -1.58, -0.15 and -0.55, 0.65 and 0.16, and -0.28 and -0.66 Gmoles day^{-1} for winter, spring, summer, and fall, respectively, with annual total exports of -0.24 and -0.65 Gmoles day^{-1}, respectively (note that negative signs represent import). This indicates that the exports of O_x and O_3 produced in the PBL to the global environment occur primarily in summer, and rarely in other seasons in 2001. The net annual positive exports occur for all other species including NO_x, NO_y, HNO_3, SO_2, AVOCs, and BVOCs, with 0.07, 0.42, 0.11, 0.07, 3.92, and 0.16 Gmoles day^{-1}, respectively. For comparison, *Liang et al.* [1998] estimated the annual mean exports of 3.8, 0.17, and 0.40 Gmoles day^{-1} for O_3, NO_x, and NO_y, respectively, based on the 1990 national emission inventory (NEI) which provides much higher emissions than the NEI 1999 version 3 used in this study. In addition to differences in emissions, the large differences in simulated exports of O_3 and NO_x between this work and that of *Liang et al.* [1998] can also be attributed to other differences of the models used in the two studies such as gas-phase chemistry and aerosol treatments. *Wang et al.* [2009] estimated the 2001 annual mean exports from the Asian and the U.S. PBL to be -0.11 and 2.04 Gmoles day^{-1} for O_3, 0.05 and 0.14 Gmoles day^{-1} for NO_x, and 0.44 and 0.62 Gmoles day^{-1} for NO_y, respectively, based on the NEI 1999 version 1 that also contains emissions higher than those used in this study. Emissions contribute to NO_x and NO_y production in all seasons, with the smallest contribution in winter but the largest one in summer. Gas-phase chemistry, cloud processes, and dry deposition are the major removal processes for NO_x and NO_y. The smallest removal occurs in winter and the largest one occurs in summer because of reduced or enhanced, respectively, photochemical activities. The differences in the net production and loss of NO_x and NO_y result in the highest net export in winter for NO_x but the highest one for NO_y in summer. For HNO_3, gas-phase chemistry and PM processes are the main contributors for its accumulation, and dry deposition and cloud processes contribute the most to its depletion. While the net production is the smallest in winter, the net loss is also the smallest in winter, resulting in the highest net export in this season. SO_2 has the highest emissions and lowest removal in winter; it has the second highest emissions and largest removal in summer, resulting in the highest net export in winter and the lowest one in summer. Emissions are the only production process for AVOCs and BVOCs; all other processes contribute to their losses. Their emissions are the highest in summer but lowest in winter, and similar seasonal trend is found for net losses, resulting in the highest net export in summer and the lowest one in winter. Compared to BVOCs that are highly

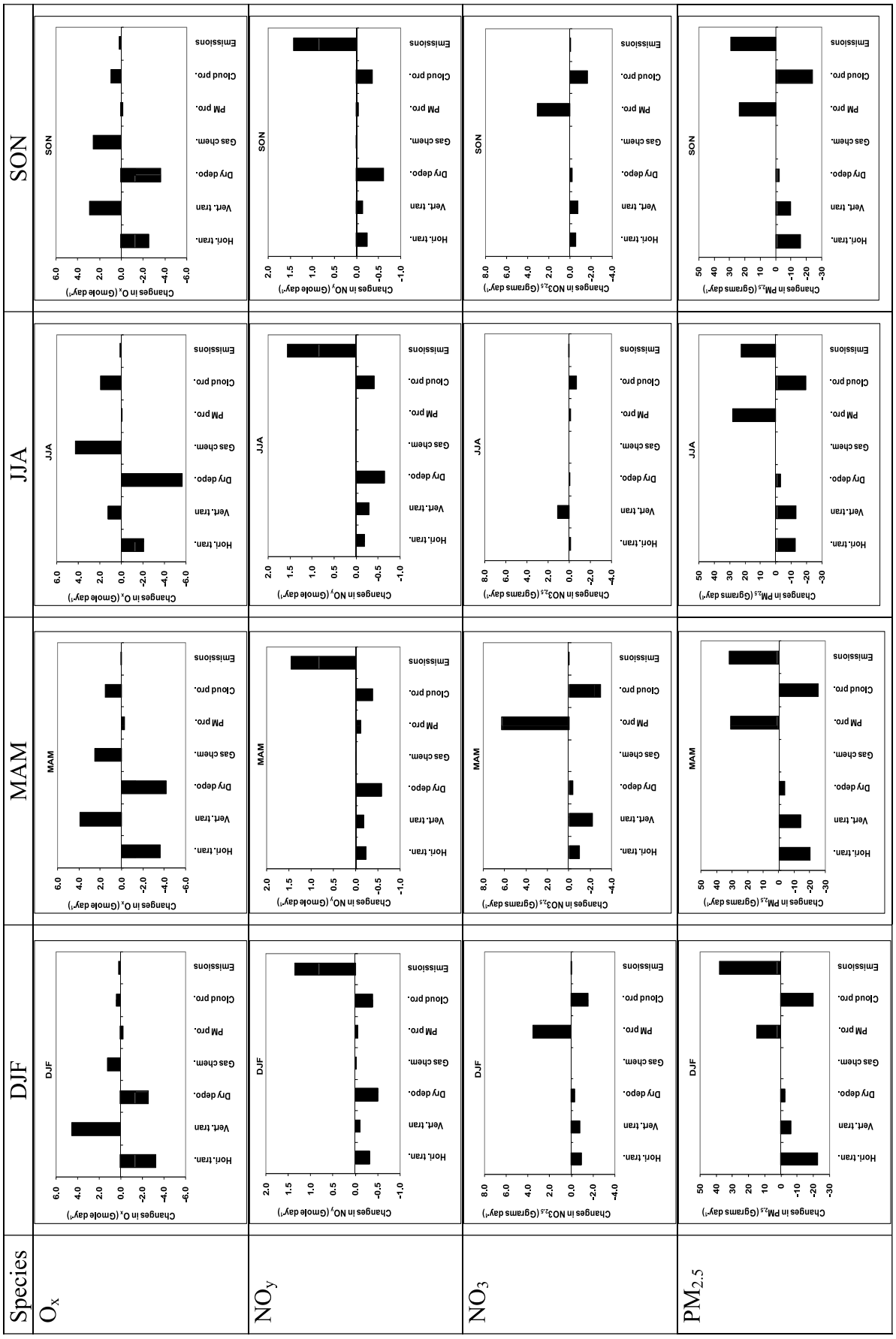

Figure 4. Seasonal mean contributions of individual processes to the changes in total O_x (Gmole day^{-1}), NO_y (Gmole day^{-1}), NO_3^- (Ggrams day^{-1}), and $PM_{2.5}$ (Ggrams day^{-1}) in the PBL in 2001.

Table 5. Total Seasonal and Annual Mean Daily Exports of Major Air Pollutants From the PBL of the United States in 2001[a]

Period	O_x	O_3	NO_x	NO_y	HNO_3	SO_2	AVOCs	BVOCs	NH_4^+	SO_4^{2-}	NO_3^-	OM	BC	OIN	$PM_{2.5}$
Winter	−1.18	−1.58	0.15	0.41	0.15	0.11	2.68	0.02	1.47	9.23	1.65	3.23	0.35	13.39	29.32
Spring	−0.15	−0.55	0.05	0.41	0.09	0.07	3.28	0.17	3.32	12.03	3.09	5.34	0.35	10.04	34.18
Summer	0.65	0.16	0.02	0.49	0.11	0.03	6.06	0.36	2.53	13.38	−0.95	6.04	0.43	5.10	26.56
Fall	−0.28	−0.66	0.06	0.39	0.10	0.06	3.66	0.11	1.66	9.33	1.35	5.14	0.31	7.78	25.68
Annual	−0.24	−0.65	0.07	0.42	0.11	0.07	3.92	0.16	2.25	10.99	1.29	4.94	0.36	9.08	28.94

[a]These values are calculated as accumulated amounts exported from the PBL of the domain, i.e., layers 1–10 (corresponding to 0–2.9 km above ground level), The unit is Gmoles/day for gases and Ggrams/day for $PM_{2.5}$ and its components. O_x, total odd oxygen; O_3, ozone; NO_x, nitrogen oxides; NO_y, total reactive nitrogen; HNO_3, nitric acid; SO_2, sulfur dioxide; AVOCs, anthropogenic volatile organic compounds (VOCs); BVOCs, biogenic VOCs; NH_4^+, ammonium; SO_4^{2-}, sulfate; NO_3^-, nitrate; OM, organic matter; BC, black carbon; OIN, other inorganic aerosols; and $PM_{2.5}$, particulate matters with aerodynamic diameter less than or equal to 2.5 μm.

reactive and thus destroyed rapidly through various oxidation reactions, AVOCs generally have weaker chemical activities and thus longer lifetimes, resulting in larger exports. For example, the lifetimes of isoprene and monoterpene against the OH reaction range from less than 1 h to 3.4 h, those for propene, xylene, formaldehydes, butane, and toluene are several hrs to several days under typical polluted urban and free tropospheric conditions [*Jacobson*, 2005; *Seinfeld and Pandis*, 2006].

[14] Net annual positive exports also occur for $PM_{2.5}$ and its major components. The net exports of $PM_{2.5}$ are 29.32, 34.18, 26.56, and 25.68 Ggrams day^{-1} for winter, spring, summer, and fall, respectively, with an annual mean export of 28.94 Ggrams day^{-1}. For comparison, *Wang et al.* [2009] estimated the 2001 annual mean exports of $PM_{2.5}$ from the Asian and the U.S. PBL to be 48.18 and 27.51 Ggrams day^{-1}, respectively. Emissions and PM processes dominate $PM_{2.5}$ accumulation, with maximum emissions occurring in winter and maximum accumulation due to PM processes occurring in spring (see Figure 4). The second highest emissions in spring coupled with the highest production from PM processes lead to the highest net $PM_{2.5}$ production throughout the year. Compared with the export of O_x that primarily occurs in summer, $PM_{2.5}$ can be exported in similar amounts out of the PBL in all seasons, indicating a need to monitor and control $PM_{2.5}$ formation throughout the year, rather than in spring and winter when the export is the highest and the second highest. The net annual exports of $PM_{2.5}$, NH_4^+, SO_4^{2-}, NO_3^-, OM, BC, and OIN, are 28.94, 2.25, 10.99, 1.29, 4.94, 0.36, and 9.08 Ggrams day^{-1}, respectively. Among them, SO_4^{2-}, OIN, and OM are the top three contributors to total annual exports of $PM_{2.5}$. PM processes are the only contributor to NH_4^+ production; all other processes contribute to its removal. The second highest production but the second highest removal in spring lead to the highest net exports of 3.32 Ggrams day^{-1} for NH_4^+. PM processes, cloud processes, and emissions are dominant contributors to SO_4^{2-} production; dry deposition contributes to its removal, in addition to wet deposition which is one of the cloud processes. The maximum production from the condensation of H_2SO_4 occurs in summer because of the strongest photochemical oxidation. The maximum production from cloud processes occurs in winter because of most abundance of clouds that serve as sites for aqueous-phase oxidation of SO_2 to produce H_2SO_4. Its maximum production from emissions also occurs in winter because of high emissions of SO_2/SO_3 to meet the highest energy/heating demands among all months. Among these, PM processes dominate, resulting in the highest SO_4^- net export in summer and the lowest in winter. NO_3^- is produced primarily from PM processes in winter, spring, and fall but destroyed by all processes except for direct emissions of nitrate (whose contribution is negligible), leading to the highest net export in spring and a negative export in summer. Similar to $PM_{2.5}$ mass, PM processes and emissions are the two major contributors to OM production, and cloud processes such as convective mixing, scavenging, and wet deposition are major contributors to its loss. The maximum accumulation occurs in summer due to the dominance of production from PM processes, and the maximum removal also occurs in summer due to the strong ventilation associated with convection clouds that may have carried some OM out of PBL to free troposphere. The highest net export for OM occurs in summer and the lowest occurs in winter. Emissions are the only contributor to both BC and OIN, with the maximum occurring in summer for BC and in winter for OIN. Cloud scavenging and wet deposition are the dominant removal processes, also with the maximum occurring in summer for BC and in winter for OIN. The maximum net export occurs in summer for BC and in winter for OIN.

4. Integrated Reaction Rates (IRRs) and Additional Indicator Analyses

4.1. Analyses of IRR Products

[15] Figure 5 shows the spatial distributions of the seasonal mean O_x production and OH chain length at surface. The production of O_x is the highest in summer, followed by fall, spring, and winter, indicating an overall higher oxidation capacity in summer and fall, which leads to higher O_3 pollution. In summer and fall, higher production occurs over several states in the western U.S. including CA, AZ, NM, CO, UT, ID, OR, MT, TX, and LA, over several states in the southeastern U.S. including FL, GA, AL, SC, and NC, as well as northern Mexico and some southern Canadian provinces such as Alberta and Saskatchewan. Unlike O_x, OH chain lengths are high in spring and winter when the VOC/NO_x ratios are relatively low and the removal of OH from the photochemical cycles are slow over nearly the entire domain. OH chain lengths decrease at low VOC/NO_x ratios due to higher NO_2 that removes OH to form HNO_3 and also at high VOC/NO_x ratios due to increased termination of RO_2 radicals that inhibit their conversion to OH radicals [*Seinfeld and Pandis*, 2006]. The lower OH chain lengths in summer and fall over most regions are attributed to increased VOC/NO_x ratios thus a faster removal of OH from photochemical cycles and increased termination of RO_2 (particularly due to much higher BVOCs in southeastern and northwestern U.S. and southern Canada in summer and fall), indicating a higher overall efficiency in

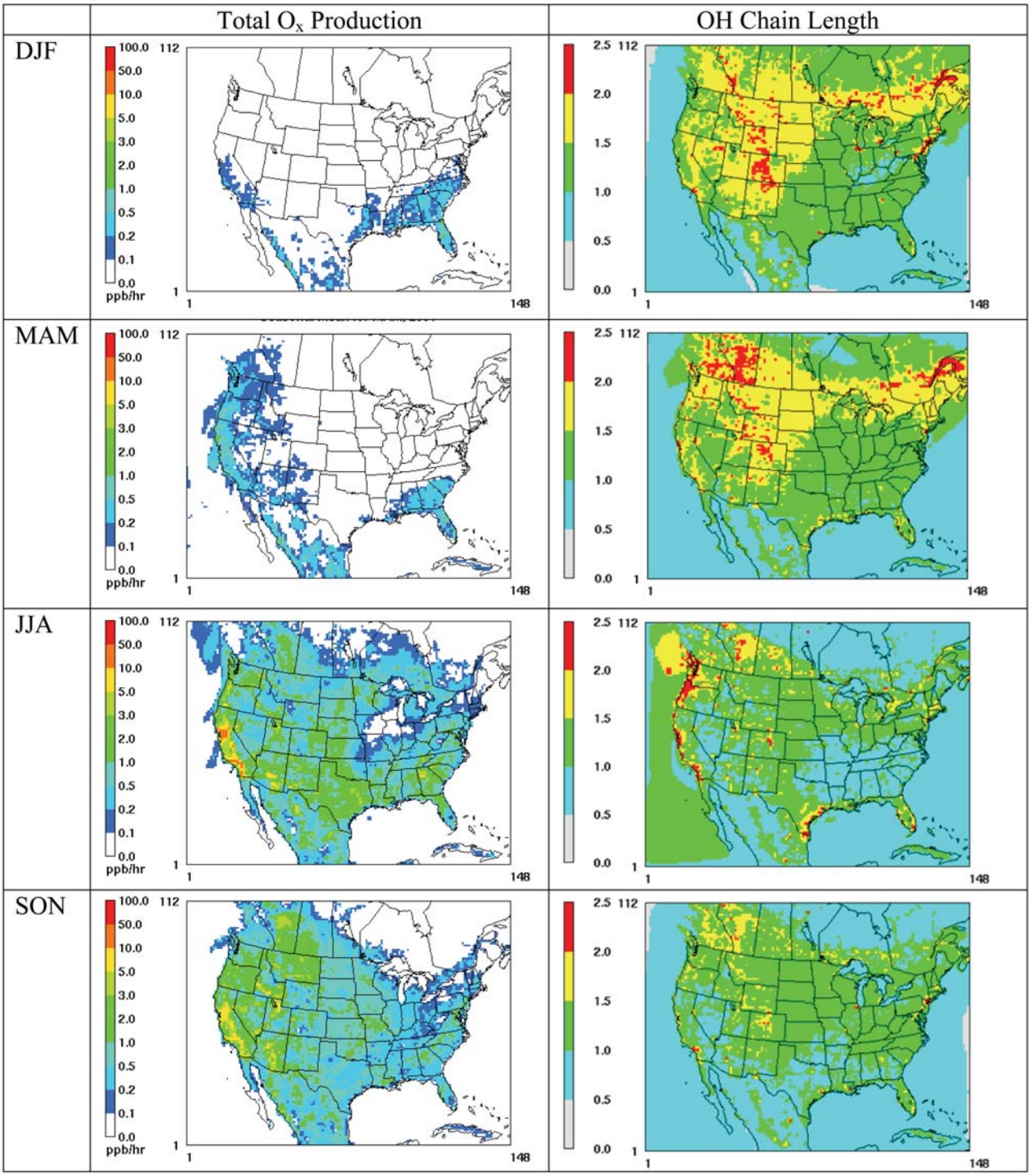

Figure 5. Seasonal mean spatial distributions of (left) total O_x production and (right) OH chain length in surface layer in 2001. DJF, December–January–February; MAM, March–April–May; JJA, June–July–August, and SON, September–October–November.

converting NO to NO_2 for O_3 formation and thus higher OH level than spring and winter, which leads to high O_3 pollution. The OH chain lengths in some coastal areas (e.g., near the west coast of the U.S., the southeastern coast of TX, and the coastal areas in FL), however, are the highest in summer. The unique VOC and NO_x emissions and meteorology (e.g., sea breeze) over these regions may lead to a chemical condition with optimal VOC/NO_x ratios that favor the OH production over its destruction (e.g., a condition with relatively low NO_2 and not too high VOCs), which slows down its removal.

[16] Table 6 summarizes the 34 IRR outputs from the CMAQ-PA tool as annual mean values at surface at the 16 locations. They provide information for the O_x budget,

Table 6. Annual Mean Values of Chemical Variables at Surface at 16 Locations[a]

IRR Outputs[b]	BBE	CHI	FRE	GRC	GRS	HOU	JST	LAX	NYC	OLY	PIT	PSU	RIV	YEL	YRK	TAM
Total O_xProd	10.9	38.0	60.8	21.9	31.4	48.4	107.0	75.4	36.4	9.3	39.0	29.7	49.1	4.7	69.1	85.8
O_xLoss	6.6	3.4	7.8	6.5	8.6	4.6	9.3	5.7	3.4	1.9	4.1	5.8	4.3	3.1	11.4	8.4
newOH_O^1D	5.1	2.8	3.2	4.4	4.9	5.5	6.0	4.4	3.0	1.0	3.5	3.3	4.2	2.0	5.9	7.1
newOHother	0.1	0.3	0.2	0.1	0.1	0.5	0.3	0.7	0.3	0.1	0.2	0.1	0.7	0.0	0.2	0.2
nwHO_2_HCHO	1.7	1.6	2.1	2.0	2.0	2.0	3.0	3.2	1.6	0.6	1.2	1.3	2.4	1.0	2.5	2.1
newHO_2tot	3.0	3.8	5.2	3.4	4.3	4.2	8.3	6.9	3.8	1.3	3.2	2.9	4.8	1.7	6.3	5.3
newRO_2tot	4.5	6.2	14.7	4.4	13.5	4.5	22.6	7.8	8.7	1.2	8.1	9.0	5.3	1.0	22.5	11.7
nHO_x_isop	0.3	0.3	1.5	0.9	1.6	0.2	1.7	0.8	0.2	0.0	0.4	1.1	0.1	0.2	2.6	1.0
OHwCO_CH_4	3.7	3.8	8.4	3.1	3.1	6.2	9.7	7.2	4.8	2.3	5.2	3.4	7.7	1.7	4.6	9.5
ISOPwOH	2.5	3.0	6.9	7.8	9.8	3.4	14.8	11.1	0.8	0.2	3.4	7.4	2.2	1.5	16.7	15.9
ISOPwO_x	0.4	0.4	1.9	1.1	2.0	0.3	2.1	1.0	0.2	0.0	0.4	1.3	0.2	0.3	3.1	1.3
OH_VOC	9.4	11.5	22.5	7.7	8.9	15.9	31.0	20.8	13.4	6.0	13.4	8.4	19.8	4.1	16.6	24.9
OHw_all_HC	12.4	15.3	31.5	16.7	20.6	20.2	50.1	34.2	14.8	6.4	17.8	17.4	22.8	5.9	37.3	44.9
OHpropmisc	0.5	0.5	0.8	0.4	0.4	0.7	0.9	0.5	0.5	0.1	0.9	0.4	0.7	0.1	0.8	1.0
HO_2TotProd	15.5	21.1	37.0	19.8	24.8	27.1	58.7	41.9	20.7	7.4	22.4	20.3	29.2	7.3	42.8	49.0
RO_2TotProd	5.8	8.1	18.1	5.5	15.1	6.7	28.3	11.1	10.9	2.2	10.1	10.3	8.3	1.6	25.9	15.4
HO_2_to_NO_2	4.7	20.0	32.0	9.9	13.7	25.9	55.0	39.9	19.6	5.1	21.2	14.0	27.6	2.2	32.1	44.2
HO_2_to_OH	7.9	20.0	33.4	12.7	16.3	25.9	55.6	40.0	19.6	5.7	21.4	15.5	27.8	3.9	34.4	45.1
RO_2_to_NO_2	6.1	17.0	27.8	11.5	16.8	21.5	49.9	33.9	15.7	4.2	17.0	15.0	20.6	2.4	35.4	39.7
OH_reacted	13.5	23.9	38.2	18.3	23.0	32.6	64.4	46.9	23.4	7.0	25.8	20.1	33.4	6.3	43.0	54.7
OHterm	0.6	8.0	6.0	1.2	2.0	11.8	13.4	12.1	8.1	0.5	7.1	2.2	9.8	0.3	4.9	8.8
HO_2term	8.0	0.0	2.9	7.2	8.4	0.1	1.2	0.3	0.1	1.5	0.3	4.7	0.3	3.6	8.0	2.6
RO_2term	0.2	0.2	0.1	0.1	0.1	0.4	0.3	0.2	0.2	0.0	0.1	0.1	0.2	0.1	0.1	0.1
H_2O_2Prod	2.5	0.0	1.0	2.2	2.6	0.0	0.5	0.1	0.0	0.6	0.1	1.5	0.2	1.1	2.5	1.0
HCHOp_isop	1.8	2.2	5.1	5.7	7.4	2.4	10.7	7.9	0.7	0.2	2.5	5.5	1.6	1.2	12.4	11.2
HCHOp_Tot	8.3	8.7	16.6	10.9	13.9	11.5	26.9	18.3	7.6	3.5	9.3	10.5	11.0	3.8	23.5	23.2
HNO_3_$OHNO_2$	0.2	7.0	4.6	0.4	0.9	10.2	10.6	10.2	7.2	0.3	6.1	1.3	8.8	0.1	2.9	6.5
HNO_3_NO_3HC	0.0	0.2	0.2	0.0	0.1	0.1	0.4	0.3	0.2	0.0	0.2	0.1	0.2	0.0	0.2	0.3
HNO_3_N_2O_5	0.0	0.0	0.0	0.0	0.0	0.0	0.0	0.0	0.0	0.0	0.0	0.0	0.0	0.0	0.0	0.0
HNO_3reacted	0.0	0.0	0.0	0.0	0.0	0.0	0.0	0.0	0.0	0.0	0.0	0.0	0.0	0.0	0.0	0.0
PANprodNet	0.0	0.1	0.0	0.0	0.0	0.4	0.1	0.1	0.2	0.0	0.0	0.0	0.1	0.0	0.0	0.0
PANlossNet	4.3	5.8	14.2	3.9	12.6	4.1	21.4	6.7	8.3	1.1	7.7	8.5	4.8	0.8	21.2	11.0
RNO_3_prod	0.3	0.9	2.2	0.8	1.4	0.9	3.4	2.1	0.8	0.2	1.0	1.2	1.0	0.1	2.9	2.6
OH Chain Length	1.2	1.9	1.8	1.8	1.5	2.3	1.9	2.4	1.8	2.0	1.8	1.7	2.2	2.0	1.6	2.3

[a]BBE, Big Bend National Park, TX; CHI, Chicago, IL; FRE, Fresno, CA; GRC, Grand Canyon National Park, AZ; GRS, Great Smoky National Park, TN; HOU, Huston, TX; JST, Jefferson Street, Atlanta, GA; LAX, Los Angeles, CA; NYC, New York City, NY; OLY, Olympic National Park, WA; PIT, Pittsburgh, PA; PSU, Pennsylvania State University, PA; RIV, Riverside, CA; YEL, Yellowstone National Park, WY; YRK, Yorkville, GA; TAM, Tampa, FL.

[b]The full names of each IRR product can be found in Table 1. The unit is ppb h^{-1} for all IRR products except for OH Chain Length which is dimensionless.

initiation, propagation, and termination of radical species, production of HCHO, termination of NO_x, and overall oxidation efficiency. The top six locations for the total photochemical reactivity, as measured by the total O_x production, Total OxProd, are JST, TAM, LAX, YRK, FRE, and RIV, with 107.0, 85.8, 75.4, 69.1, 60.8, and 49.1 ppb of daily O_x production. Radical initiation is the key chemical process that limits O_3 formation for VOC-sensitive conditions; its major sources include the reaction of O^1D with H_2O (i.e., newOH_O^1D), photolysis of HCHO (i.e., newHO_2_HCHO), and the photolysis of carbonyls and reactions of organic compounds that produces HO_2 (i.e., newHO_2tot). High newOH_O^1D production occurs at TAM, JST, YRK, HOU, BBE, and GRS. High newHO_2tot production occurs at JST, LAX, YRK, TAM, FRE, and RIV, resulting in high O_x production at those locations. Radical propagation is another indicator of the overall photochemical reactivity. For example, the amount of total HO_2 production, HO2TotProd, is relatively high at JST, TAM, YRK, LAX, FRE, and RIV. The contributions of BVOCs and AVOCs can be estimated qualitatively by comparing the amount of CO, CH_4, VOCs, and isoprene reacted at each location. For example, the contribution of isoprene, ISOPwOH, is relatively high at YRK, TAM, JST, LAX, GRC, PSU, and FRE and the contributions of AVOCs (i.e., OH_VOC) and total VOCs (i.e., OHw_all_HC = OH reacting with AVOCs and BVOCs) are relatively high at JST, TAM, FRE, LAX, RIV, YRK, HOU, NYC, PIT, and CHI. Figure 6 compares the rates of OH reacting with AVOCs and BVOCs in the surface layer at four urban sites (i.e., CHI, LAX, JST, and NYC), a suburban site (i.e., RIV), and a rural site (i.e., YRK). The highest rates of OH reacted with both AVOCs and BVOCs occur at JST. The rate of OH reacted with BVOCs is even higher than that with AVOCs at YRK during summertime. Among the 16 sites, JST has the highest O_3 and O_x formation (Figure not shown). The contribution of BVOCs to O_3/O_x formation at JST, YRK, and TAM is reflected by high contributions of gas-phase chemistry to O_3 production during summer months at both sites as shown in Figure 1. Nearly the same rates of OH reacted with both AVOCs and BVOCs at LAX, whereas the rate of OH reacted with BVOCs is much smaller than that with AVOCs at RIV, reflecting much lower BVOCs emissions at RIV. The rate of OH reacted with AVOCs is much stronger than that with BVOCs at CHI and NYC. The seasonal and annual rates of OH reacted with BVOCs are the lowest at NYC among the four urban locations. Several IRR products such as NO_2 produced from reactions of HO_2 (HO_2_to_NO_2), OH produced from reactions of HO_2 (HO_2_to_OH), and total OH production (OH_reacted) give

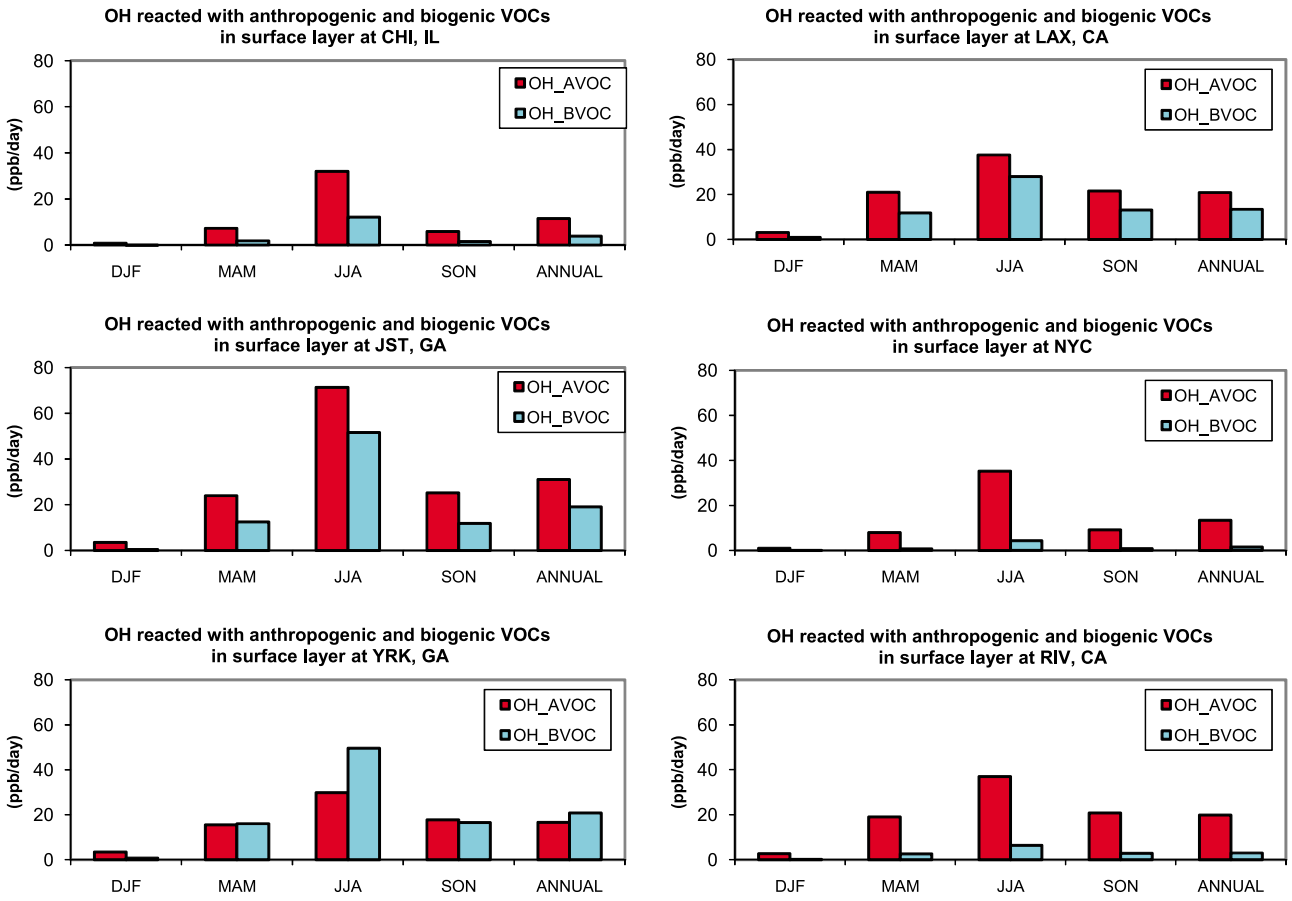

Figure 6. Seasonal and annual mean rates of OH reacted with anthropogenic and biogenic VOCs at Chicago (CHI), IL; Los Angeles (LAX), CA; Jefferson Street (JST), Atlanta, GA; New York City (NYC); Yorkville (YRK), GA, and Riverside (RIV), CA in 2001.

the top 10 sites with a ranking identical to that of O_x chemical production (Total O_xProd) (i.e., from the highest to the lowest: JST, TAM, LAX, YRK, FRE, RIV, HOU, PIT, CHI, and NYC); all of which can be used to collectively indicate the overall oxidation efficiencies of the atmosphere over those sites.

[17] OH chain length is an indicator for overall oxidation efficiency. The values of OH chain lengths at LAX, HOU, TAM, RIV, OLY, and YEL are 2.0–2.4, those at JST, CHI, FRE, GRC, NYC, PIT, PSU, and YRK are 1.6–1.9, and those at GRS and BBE are 1.2–1.5. The OH chain lengths are relatively high at sites near the coast for the same reason stated previously, and relatively low at national parks GRS and BBE where VOC/NO_x ratios are very low, a condition that favors the removal of OH through its reaction with NO_2 to form HNO_3. The magnitudes of the OH chain lengths at those sites provide a relative measure of the overall efficiency in converting NO to NO_2 for O_3 formation on an annual basis. For example, the OH chain length of 1.2 at BBE is a factor of 2 shorter than that at LAX, indicating that NO can be converted to NO_2 to produce O_3 twice more efficiently than that at LAX on an annual basis, despite much lower NO_x mixing ratios at BBE, as compared with those at LAX.

4.2. Analyses of Chemical Indicators

4.2.1. Sensitivity of O_3 to Its Precursors

[18] P_{H2O2}/P_{HNO3} is a useful indicator for O_3 photochemistry that can be calculated using the net productions of H_2O_2 and HNO_3 from IRR products (i.e., H_2O_2Prod and the sum of HNO_3_$OHNO_2$, HNO_3_NO_3HC, and HNO_3_N_2O_5 in Table 1, respectively). As shown in Figure 7, the monthly mean ratios of $PH_2O_2/PHNO_3$ are below 0.2 during January, February, and December in most areas except for some areas in a few states in the western U.S. (e.g., NV, OR, ID, MT, WY, AZ, NM, UT, and CO), indicating a VOC-limited O_3 chemistry. Some states in the central plains (e.g., SD, NE, KS, OK, and TX) experience a transition from VOC-limited to NO_x-limited conditions in March. However, many areas in CA and WA especially those over major cities (e.g., Los Angles, San Francisco, and Seattle) are VOC-limited throughout January–March and December due to high NO_x emissions and relatively low BVOCs emissions. In April and May, almost all areas except for small areas in OH, MI, northern IN and IL, DC, MD, DE, NJ, CT, RI, and MA and several metropolitan areas (e.g., San Francisco, LAX, and Minneapolis) become NO_x-limited with ratios of $P_{H2O2}/P_{HNO3} \geq 0.4$. While major cities (e.g., San Francisco, LAX, CHI, Cleveland, Cincinnati, NYC,

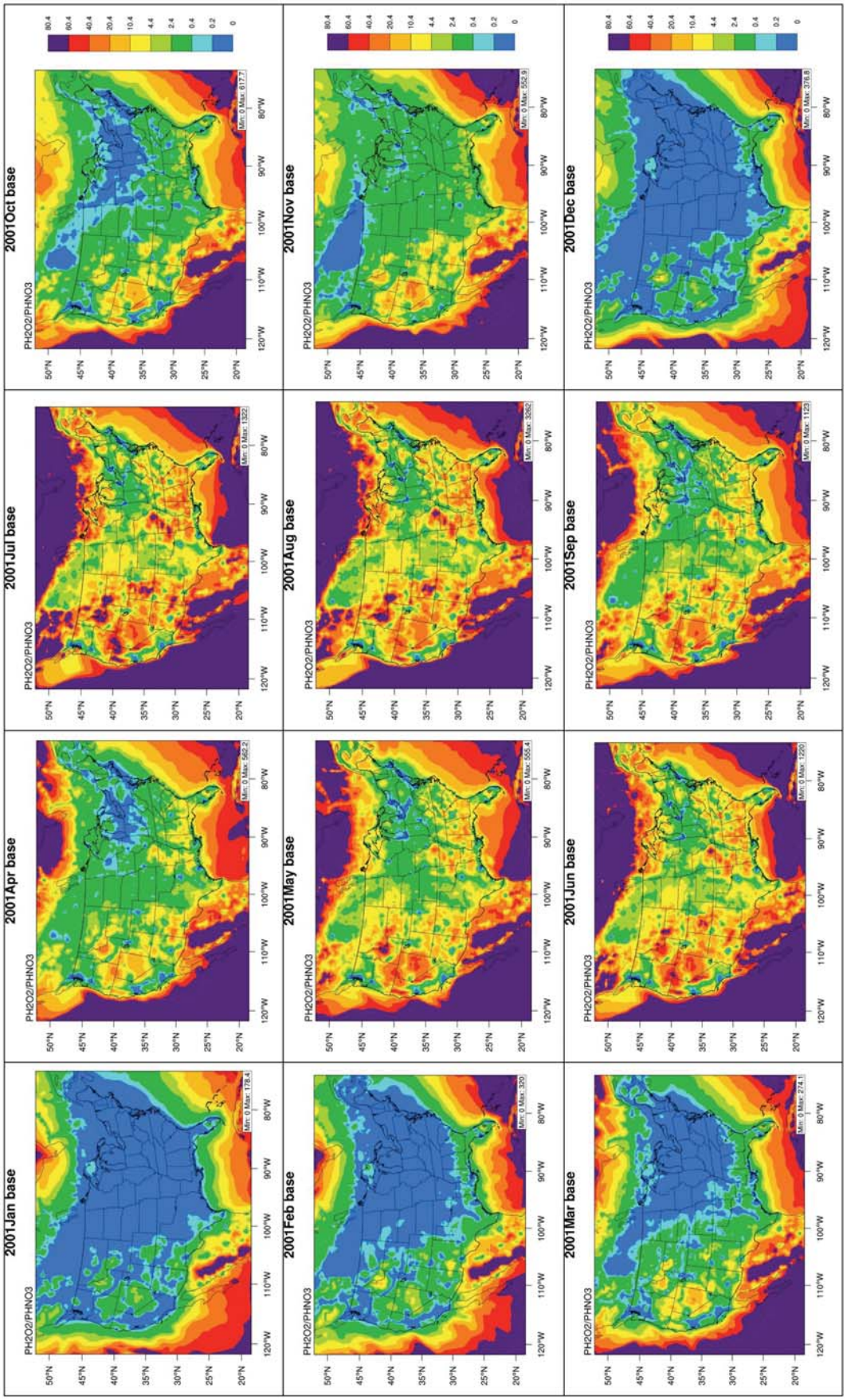

Figure 7. Simulated monthly mean ratios of production rates of H_2O_2 and HNO_3 (P_{H2O2}/P_{HNO3}) from the integrated reaction rates (IRR) of the process analysis in 2001.

Baltimore, Philadelphia, and Atlanta) remain VOC-limited in the remaining months, all other areas are NO_x-limited with the largest NO_x-limited extent (based on the highest ratio of P_{H2O2}/P_{HNO3} among all months) in July. One exception occurs in October over some areas in some states in the Middle West and northeastern U.S. where O_3 chemistry switches from NO_x-limited in September to VOC-limited in October, then changes back to NO_x-limited in November, indicating a high sensitivity of O_3 chemistry to the ratios of VOCs and NO_x emissions and possibly a chemical condition along the ridge line at which O_3 chemistry is equally sensitive to NO_x and VOCs. These results are overall consistent with VOC- versus NO_x-limited O_3 chemistry reported in the literature [e.g., *Chameides et al.*, 1988, 1997; *Lindsay et al.*, 1989; *Pun and Seigneur*, 2001; *Sillman and He*, 2002; *Zhang et al.*, 2005, 2009]. They also indicate a need to use different control strategies for areas with opposite O_3 sensitivity in summer.

[19] To verify the robustness of P_{H2O2}/P_{HNO3} as an indicator for sensitivity of O_3, P. Liu et al. (Use of a process analysis tool for diagnostic study on fine particulate matter predictions in the U.S. Part II: Process Analyses and Sensitivity Simulations, submitted to *Atmospheric Environment,* 2009) conducted two separate sensitivity simulations, with 50% reductions in NO_x emissions or anthropogenic VOC emissions for a summer episode. The simulated responses of O_3 mixing ratios to changes in the emissions of NO_x and VOCs using such a brute force method were found to be fairly consistent with the sensitivity of O_3 identified by P_{H2O2}/P_{HNO3}. Given its robustness, P_{H2O2}/P_{HNO3} is thus used as a benchmark in this study to judge the appropriateness of the transition values of other indicators reported in the literature, which are adjusted if such values provide an inconsistent O_3 sensitivity with that indicated by P_{H2O2}/P_{HNO3}. While P_{H2O2}/P_{HNO3} has been considered to be a robust indicator for local sensitivity of O_3 [*Tonnesen and Dennis*, 2000a; Liu et al., submitted manuscript, 2009], other indicators have also been used to verify the simulated O_3 sensitivity. Figure 8 shows the afternoon mean values between noon to 6 P.M. LST for 8 indicators in January and August. The values of $H_2O_2/(O_3 + NO_2)$, $HCHO/NO_y$, and $HCHO/NO_z$ are lower than the reported transition values of 0.02, 0.28, and 1, respectively, over most of areas in January, indicating a VOC-limited O_3 chemistry which is consistent with the results based on P_{H2O2}/P_{HNO3}. The values of H_2O_2/HNO_3 are lower than the reported transition value of 0.2 only in the northeastern U.S., those of NO_y are greater than the reported transition value of 20 ppb in some areas in the northeastern U.S., the values of O_3/NO_x are lower than the reported transition value of 15 over the eastern U.S., the values of O_3/NO_y are lower than the reported transition value of 7 in the eastern U.S., partially consistent with the results based on P_{H2O2}/P_{HNO3} over those areas. None of the values of O_3/NO_z are lower than the reported transition value of 7, indicating an opposite O_3 sensitivity simulated using O_3/NO_z values (i.e., NO_x-limited) in January. In August, the values of H_2O_2/HNO_3, $H_2O_2/(O_3 + NO_2)$, O_3/NO_x, O_3/NO_y, O_3/NO_z, $HCHO/NO_y$, and $HCHO/NO_z$ are higher than 2.4, 0.04, 25, 7, 7, 0.42, and 1 (which are higher or equal to their corresponding transition values), respectively, and those of NO_y are lower than 10 ppb over most of the domain, indicating a NO_x-limited O_3 chemistry which is consistent with the results based on P_{H2O2}/P_{HNO3} over those areas. However, among all indicators, only $HCHO/NO_y$ and $HCHO/NO_2$ are able to predict VOC-limited O_3 chemistry over the aforementioned areas (e.g., the Middle West and northeastern U.S.) and major metropolitan areas (e.g., LAX, San Francisco, Seattle, CHI, NYC) where P_{H2O2}/P_{HNO3} predicts a VOC-limited O_3 chemistry based on the reported transition value of 0.2 shown in Table 2. Adjusting the transition values from 0.2 to 2.4 for H_2O_2/HNO_3, from 20 to 5 for NO_y, from 15 to 60 for O_3/NO_x, from 7 to 15 for O_3/NO_y will allow these indicators to predict O_3 sensitivity consistent with that predicted by P_{H2O2}/P_{HNO3}, $HCHO/NO_y$, and $HCHO/NO_2$ in both months. For $H_2O_2/(O_3 + NO_2)$ and O_3/NO_z, different transition values are needed in January and August to bring the indicated O_3 sensitivity more in line with other indicators. The transition value of $H_2O_2/(O_3 + NO_2)$ will need to be adjusted from 0.02 in January to 0.04 in August and that of O_3/NO_z will need to be adjusted from 7 to 100 and 20 for in January and August, respectively. Such adjustments can be justified, as the original transition values are developed based on limited point-wise measurements or model results at a smaller horizontal grid size (e.g., at 12 km by *Lu and Chang* [1998]; at 20 km by *Tonnesen and Dennis* [2000b]; and at 2–4 km by *Hammer et al.* [2002]), rather than at 36 km in this study. For comparison, *Lu and Chang* [1998] also suggested adjusted values for NO_y, $HCHO/NO_y$, H_2O_2/HNO_3, and O_3/NO_z of 4–5 ppb, 0.5–0.7, 0.8–1.0, and 25–30, respectively, based on a 3-D model simulation of a 5 day summer episode in the San Joaquin Valley, CA.

[20] Figure 9 show the afternoon mean values of those indicators at four sites: CHI, LAX, HOU, and PSU in August. The horizontal lines represent the transition values above which for NO_y and below which for remaining indicators indicate a VOC-limited O_3 chemistry. In August, NO_y, O_3/NO_x, O_3/NO_y, $HCHO/NO_y$, and $HCHO/NO_2$ are robust indicators for VOC-limited chemistry at CHI and HOU. H_2O_2/HNO_3 and O_3/NO_z indicate NO_x-limited chemistry and $H_2O_2/(O_3 + NO_2)$ indicates more days with NO_x-limited chemistry than days with VOC-limited chemistry. Adjusted transition values of 2.4, 20, and 0.04 for H_2O_2/HNO_3, O_3/NO_z, and $H_2O_2/(O_3 + NO_2)$, respectively, will bring the O_3 sensitivity more in line with other indicators. At LAX, O_3/NO_x, O_3/NO_y, $HCHO/NO_y$, $HCHO/NO_2$, and NO_y are robust indicators for VOC-limited chemistry. Adjusted transition values of 2.4 for H_2O_2/HNO_3, 0.04 for $H_2O_2/(O_3 + NO_2)$, and 20 for O_3/NO_z ensure the indicated O_3 sensitivity consistent with other indicators. At PSU, NO_y values are below 20 ppb (also below adjusted transition value of 5 ppb) and those of H_2O_2/HNO_3, O_3/NO_x, O_3/NO_y, O_3/NO_z, $HCHO/NO_y$, and $HCHO/NO_2$ are above their transition values during most of hours, indicating a NO_x-limited chemistry. The transition value of $H_2O_2/(O_3 + NO_2)$ needs to be adjusted from 0.02 to 0.01 to bring the indicated O_3 sensitivity more in line with results from other indicators. In January (Figure not shown), NO_y values are above 20 ppb and all other indicators except for H_2O_2/HNO_3 and O_3/NO_z are below their respective transition values at CHI and HOU, denoting a VOC-limited chemistry. At LAX, $NO_y \leq 20$ ppb occur on more days than $NO_y > 20$ ppb, indicating a dominance of NO_x-limited chemistry. Other

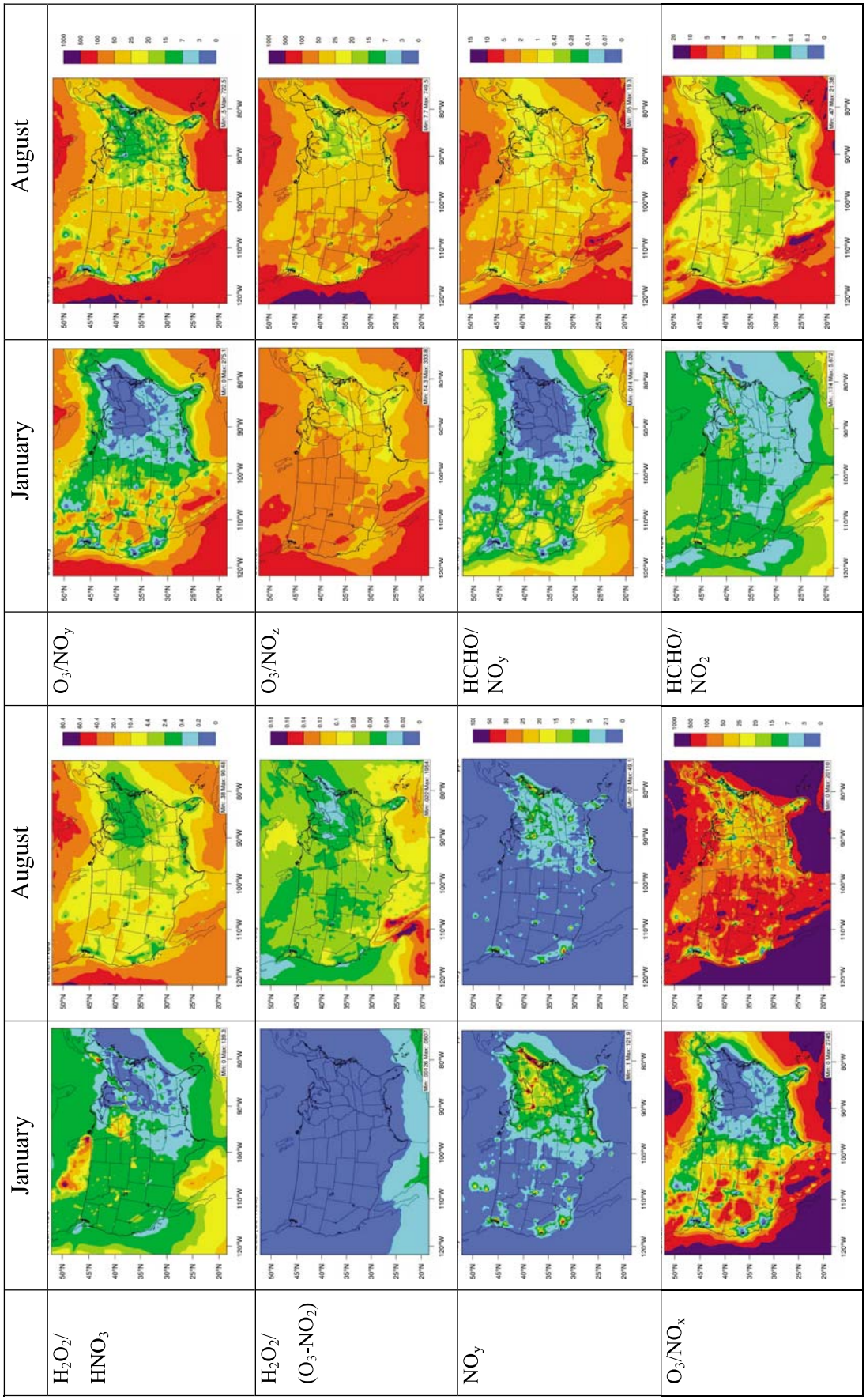

Figure 8. Simulated monthly mean spatial distributions of 8 indicators in January and August in 2001.

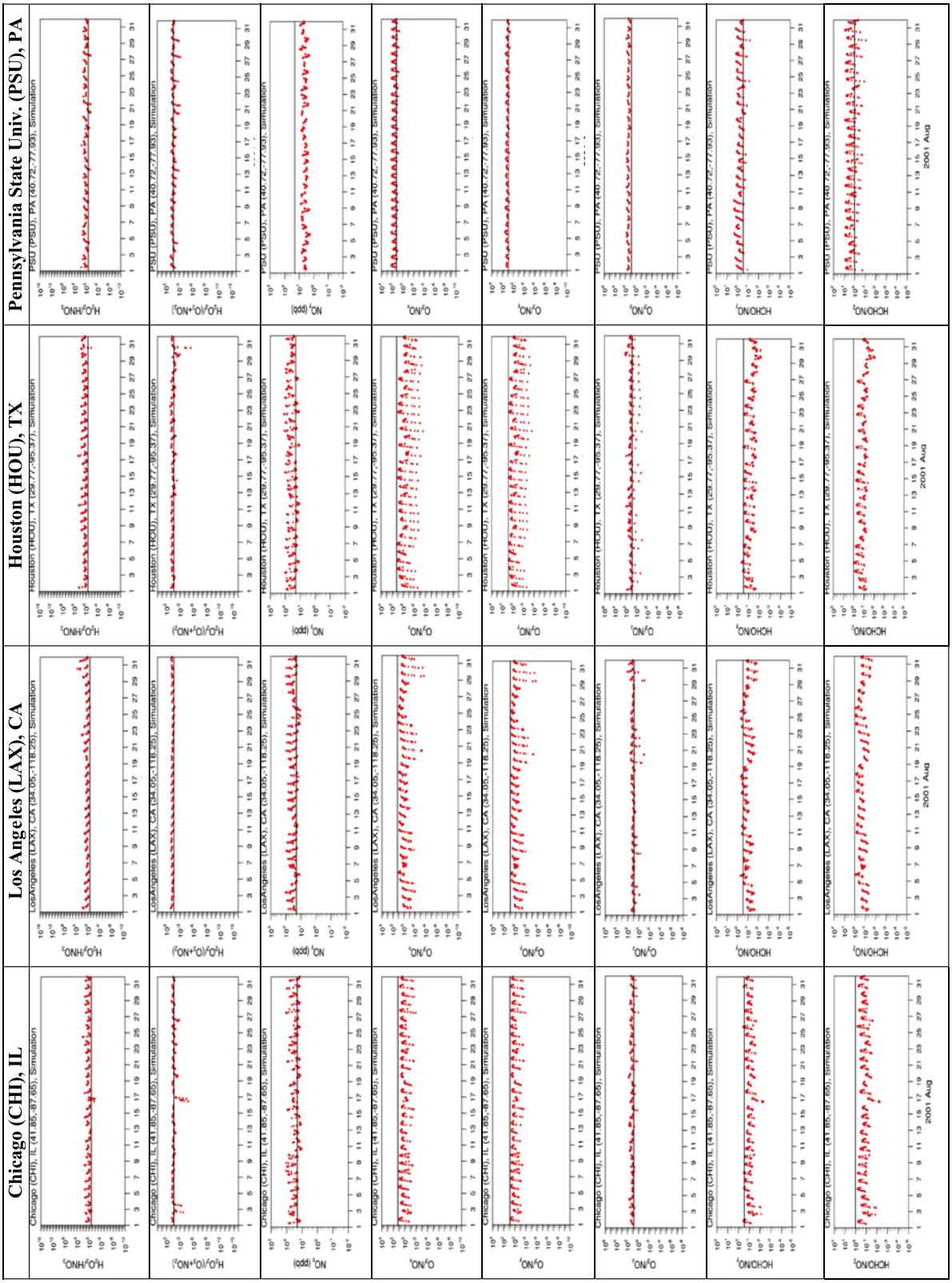

Figure 9. Simulated afternoon (between noon and 6 P.M. LST) indicators in August 2001 at 4 sites: Chicago (CHI), IL, Los Angeles (LAX), CA, Houston (HOU), TX, and Pennsylvania State University (PSU), PA. The horizontal lines represent the transition values above which for NO_y and below which for remaining indicators indicate a VOC-limited O_3 chemistry.

Table 7. NO_x- or VOC-Sensitive O_3 Chemistry at 16 Locations in January and August 2001[a]

Indicators	BBE	CHI	FRE	GRC	GRS	HOU	JST	LAX	NYC	OLY	PIT	PSU	RIV	YEL	YRK	TAM
								January								
P_{H2O2}/P_{HNO3}	NO_x	VOC	VOC	NO_x	VOC	VOC	VOC	VOC	VOC	VOC	VOC	VOC	VOC	NO_x	VOC	VOC
H_2O_2/HNO_3	NO_x	NO_x	NO_x	NO_x	VOC	NO_x	NO_x	NO_x	NO_x	ridge	NO_x	VOC	NO_x	NO_x	NO_x	NO_x
$H_2O_2/(O_3 + NO_2)$	VOC	VOC	VOC	VOC	VOC	VOC	VOC	VOC	VOC	VOC	VOC	VOC	VOC	VOC	VOC	VOC
NO_y	NO_x	VOC	NO_x	NO_x	NO_x	VOC	VOC	NO_x	VOC	NO_x	VOC	NO_x	NO_x	NO_x	NO_x	NO_x
O_3/NO_x	NO_x	VOC	VOC	NO_x	VOC	VOC	VOC	VOC	VOC	ridge	VOC	VOC	VOC	NO_x	VOC	VOC
O_3/NO_y	NO_x	VOC	VOC	NO_x	VOC	VOC	VOC	VOC	VOC	NO_x	VOC	VOC	VOC	NO_x	VOC	VOC
O_3/NO_z	NO_x	VOC	NO_x	NO_x	NO_x	VOC	ridge	NO_x	VOC	NO_x	VOC	NO_x	NO_x	NO_x	NO_x	NO_x
$HCHO/NO_y$	NO_x	VOC	VOC	NO_x	VOC	VOC	VOC	VOC	VOC	VOC	VOC	VOC	VOC	NO_x	VOC	VOC
$HCHO/NO_2$	NO_x	VOC	VOC	ridge	VOC	VOC	VOC	VOC	VOC	VOC	VOC	VOC	VOC	NO_x	VOC	VOC
Overall	NO_x	VOC	VOC	NO_x	VOC	VOC	VOC	VOC	VOC	mix	VOC	VOC	VOC	NO_x	VOC	VOC
								August								
P_{H2O2}/P_{HNO3}	NO_x	VOC	NO_x	NO_x	NO_x	VOC	VOC	VOC	VOC	NO_x	VOC	NO_x	VOC	NO_x	NO_x	VOC
H_2O_2/HNO_3	NO_x	NO_x	NO_x	NO_x	NO_x	NO_x	NO_x	NO_x	NO_x	NO_x	NO_x	NO_x	NO_x	NO_x	NO_x	NO_x
$H_2O_2/(O_3 + NO_2)$	NO_x	ridge	NO_x	NO_x	NO_x	NO_x	ridge	ridge	ridge	NO_x	ridge	ridge	ridge	ridge	ridge	ridge
NO_y	NO_x	VOC	NO_x	NO_x	NO_x	VOC	VOC	VOC	VOC	NO_x	ridge	NO_x	VOC	NO_x	NO_x	NO_x
O_3/NO_x	NO_x	VOC	ridge	NO_x	NO_x	VOC	VOC	VOC	VOC	NO_x	VOC	NO_x	VOC	NO_x	ridge	VOC
O_3/NO_y	NO_x	VOC	ridge	NO_x	NO_x	VOC	VOC	VOC	VOC	NO_x	VOC	NO_x	VOC	NO_x	ridge	VOC
O_3/NO_z	NO_x	VOC	NO_x	NO_x	NO_x	ridge	NO_x	ridge	ridge	NO_x	NO_x	NO_x	NO_x	NO_x	NO_x	NO_x
$HCHO/NO_y$	NO_x	VOC	NO_x	NO_x	NO_x	VOC	VOC	VOC	VOC	NO_x	VOC	NO_x	VOC	NO_x	NO_x	VOC
$HCHO/NO_2$	NO_x	VOC	ridge	NO_x	NO_x	VOC	VOC	VOC	VOC	NO_x	VOC	NO_x	VOC	NO_x	NO_x	VOC
Overall	NO_x	VOC	NO_x	NO_x	NO_x	VOC	VOC	VOC	VOC	NO_x	VOC	NO_x	VOC	NO_x	NO_x	VOC

[a]BBE, Big Bend National Park, TX; CHI, Chicago, IL; FRE, Fresno, CA; GRC, Grand Canyon National Park, AZ; GRS, Great Smoky National Park, TN; HOU, Huston, TX; JST, Jefferson Street, Atlanta, GA; LAX, Los Angeles, CA; NYC, New York City, NY; OLY, Olympic National Park, WA; PIT, Pittsburgh, PA; PSU, Pennsylvania State University, PA; RIV, Riverside, CA; YEL, Yellowstone National Park, WY; YRK, Yorkville, GA; TAM, Tampa, FL. NO_x and VOC indicate NO_x- and VOC-sensitive O_3 chemistry at a specific location; ridge indicates that O_3 chemistry is in the ridge zone, i.e., equally sensitive to NO_x and VOCs; mix indicates that the analysis of 8 indicators does not provide a consistent indication of O_3 chemistry, i.e., could be either NO_x or VOC chemistry.

indicators except for H_2O_2/HNO_3 and O_3/NO_z are below their transition values, indicating a VOC-limited chemistry. Using adjusted transition values of 5 ppb for NO_y, 2.4 for H_2O_2/HNO_3, and 100 for O_3/NO_z permits these indicators to denote a VOC-limited chemistry for most days, more consistent with other indicators. At PSU, $NO_y \leq 20$ ppb occur on nearly all days except on January 8, 10, 20, and 24, indicating a NO_x-limited chemistry. Other indicators except for H_2O_2/HNO_3 and O_3/NO_z are below their transition values, denoting a VOC-limited chemistry. Values of NO_y, H_2O_2/HNO_3, and O_3/NO_z relative to their adjusted transition values denote a VOC-limited chemistry that is consistent with other indicators.

[21] Table 7 summarizes the O_3 sensitivity based on afternoon mean values of 9 indicators at the 16 sites. In January, VOC-limited chemistry dominates at 12 urban, suburban, and rural sites, NO_x-limited chemistry dominates at 3 national park sites (i.e., BBE, GRC, and YEL), and no clear chemical regime can be determined at one national park site that is affected by complex coastal meteorology (i.e., OLY). Compared with results from other indicators, different O_3 sensitivity is predicted by H_2O_2/HNO_3 at all sites except for BBE, GRC, GRS, PSU, and YEL, by $H_2O_2/(O_3 + NO_2)$ at BBE and GRC, by NO_y at FRE, GRS, LAX, PSU, RIV, and YRK, and TAM, by O_3/NO_z at FRES, GRS, JST, PSU, RIV, YRK, and TAM, and by $HCHO/NO_2$ at GRC. Adjusted transition values for those indicators at those sites can ensure the indicated O_3 sensitivity consistent with other indicators. In August, VOC-limited chemistry remains dominant at 8 urban and suburban sites, NO_x-limited chemistry dominates at 1 urban site (i.e., FRE), 2 rural sites (i.e., PSU and YRK), and 5 national park sites (i.e., BBE, GRC, GRS, OLY, and YEL). Although the mixing ratios of BVOCs are high at JST, they are destroyed rapidly by available OH radicals. On the other hand, high mixing ratios of NO_2 lead to a high production of HNO_3 and the conversion of HO_2 radicals to OH radicals via its reaction with NO that dominates over its termination via its self-destruction that produces H_2O_2 (see Table 7), resulting in a VOC-limited O_3 chemistry at JST. Compared with results from other indicators, different O_3 sensitivity is predicted by H_2O_2/HNO_3 at all sites except for BBE, GRC, GRS, OLY, PSU, YEL, and YRK, by $H_2O_2/(O_3 + NO_2)$ at all sites except for BBE, GRC, GRS, and OLY, by NO_y at FRE, PIT, and TAM, by O_3/NO_z at FRE, HOU, JST, LAX, NYC, PIT, RIV, and TAM, and by $HCHO/NO_y$ at FRE. Similar to January, adjusted transition values for those indicators at those sites can bring the indicated O_3 sensitivity more in line with other indicators. As shown by *Zhang et al.* [2009], the observed indicators calculated using SEARCH data indicate a VOC-limited chemistry in January at JST and YRK and a NO_x-limited chemistry at YRK but a VOC-limited chemistry at JST in August. The simulated indicator values are overall consistent with observations, with P_{H2O2}/P_{HNO3}, NO_y, $HCHO/NO_y$, and $HCHO/NO_z$ as most robust indicators.

4.2.2. Sensitivity of $PM_{2.5}$ to Its Precursors

[22] The sensitivity of $PM_{2.5}$ to its precursors depends on the complex interplay between meteorological and chemical conditions and the dominance of precursor emissions and/or concentrations and the resulting competition among them. For inorganic PM, the thermodynamic equilibrium among NH_4^+, SO_4^{2-}, and NO_3^- affects largely the sensitivity of $PM_{2.5}$ to the emissions of SO_2, NO_x, and NH_3 as well as the resulting NH_4^+, SO_4^{2-}, and NO_3^- in the gas and particulate phases. Figure 10 shows spatial distributions of NH_4^+,

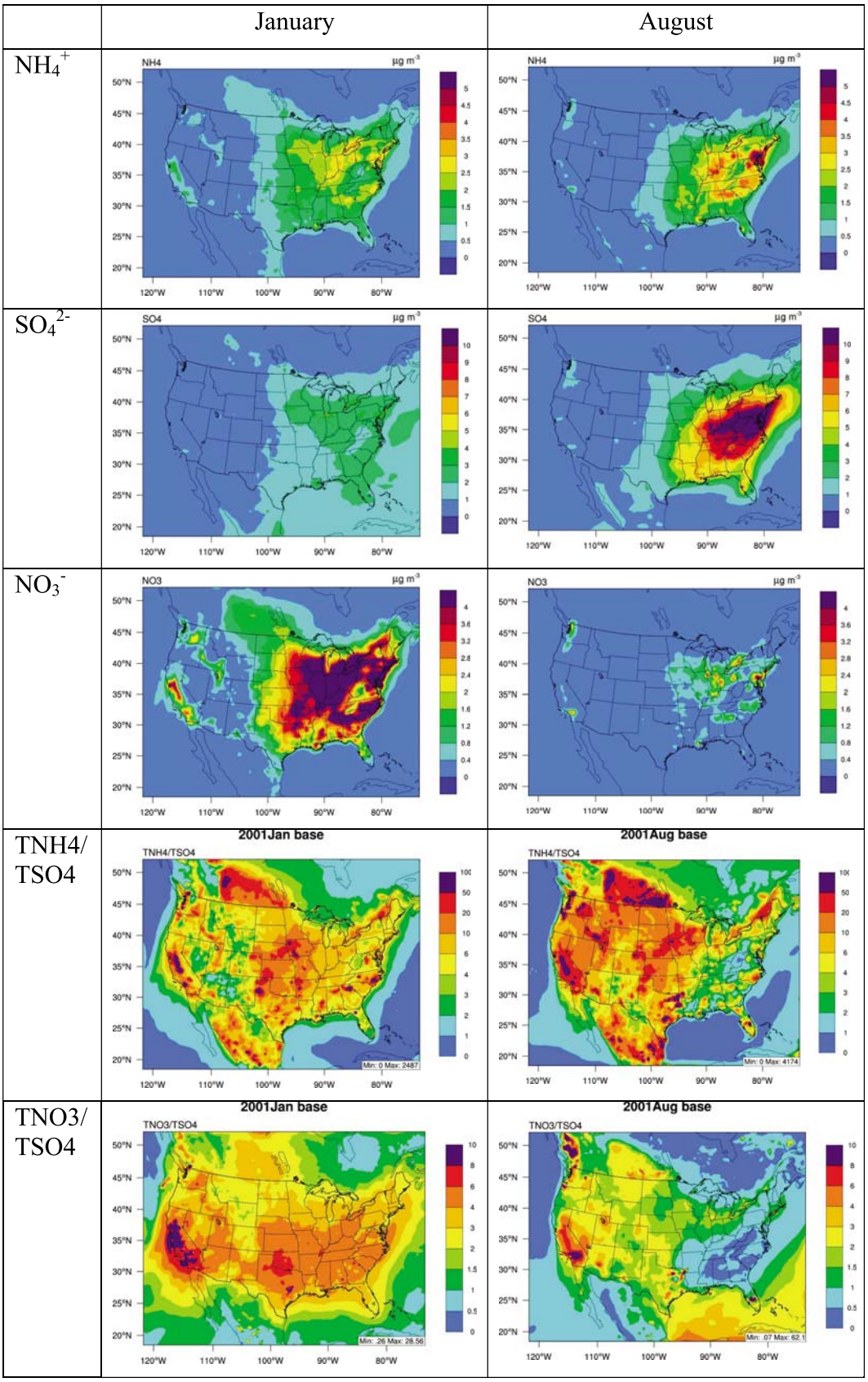

Figure 10. Simulated monthly mean spatial distributions of NH_4^+, SO_4^{2-}, NO_3^-, TNH4/TSO4, and TNO3/TSO4 in January and August 2001.

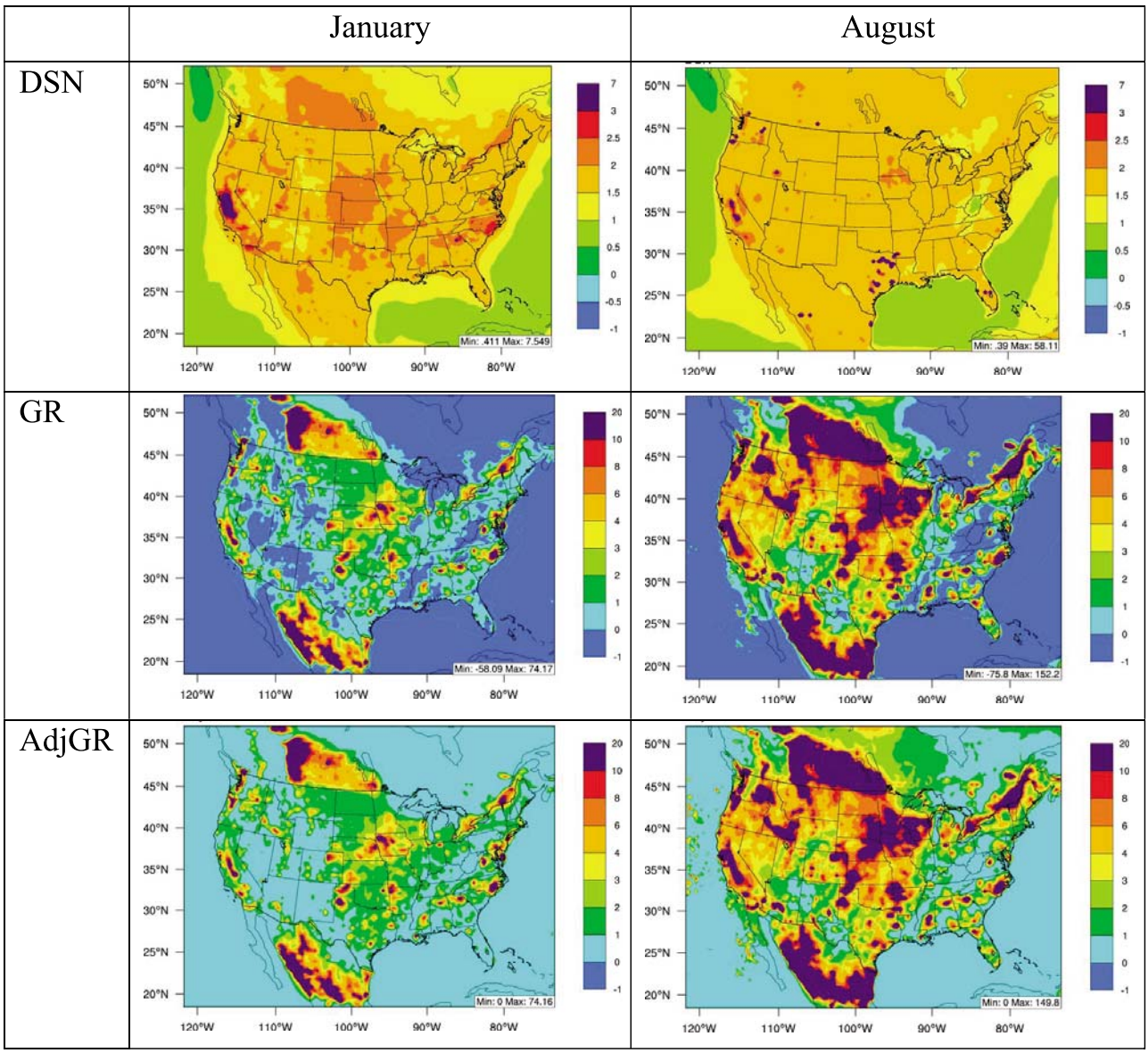

Figure 11. Simulated spatial distributions of the degree of sulfate neutralization (DSN), the gas ratio (GR), and the adjusted gas ratio (AdjGR) in January and August 2001.

SO_4^{2-}, and NO_3^-, and two ratios that provide insights into $PM_{2.5}$ formation including the molar ratios of total ammonium to total sulfate (i.e., TNH4/TSO4) and those of total nitrate to total sulfate (i.e., TNO3/TSO4), where TNH4 = $NH_3 + NH_4^+$ and TNO3 = $HNO_3 + NO_3^-$. In January, SO_4^{2-} is an important component in the eastern U.S. and NH_4NO_3 dominates most of the domain. In August, $(NH_4)_2SO_4$ dominates most of the domain, NH_4NO_3 dominates southern CA and Pacific Northwest, and both salts dominate several areas including CHI, IL, Ft. Wayne, IN, Dayton and Canton, OH, Philadelphia, PA, and Toronto, ON. Values of TNH4/TSO4 of <2, 2, and >2 indicate sulfate-rich, neutral, and poor conditions, respectively, and values of TNO3/TSO4 of <1, 1–2, and >2 indicate nitrate-poor, -medium, and -rich conditions, respectively. Values of TNH4/TSO4 are above 2 in both months over most of the domain except for some areas in AZ, NM, NV, and WA in January and WV and some areas in PA, VA, KY, OH, TN, NC, LA, MS, AL, GA, and SC, indicating a condition favoring the formation of NH_4NO_3, particularly in areas with values of greater than 6 where NH_3 is very rich (e.g., CA, central plains, Middle West, and southeastern U.S. in January and most of the western U.S. and some areas in the eastern U.S. in August). The values of TNO3/TSO4 > 2 over nearly all the domain coupled with cold T in January favor NH_4NO_3 formation. By contrast, values of TNO3/TSO4 > 2 only occur in some areas in the western U.S. and central plains in August, indicating a low-to-poor NO_3^- condition, particularly in many southern states and middle Atlantic states where TNO3/TSO4 < 1.

[23] Figure 11 shows spatial distributions of three PM chemistry indicators including DSN, GR, and AdjGR for sensitivity of $PM_{2.5}$ formation to its precursors. Full sulfate neutralization with DSN $\geq$ 2 occurs only in some areas in several states (e.g., CA, NE, KS, CO, TX, AR, and NC) in January and even fewer areas (e.g., CA, WA, MN, TX, and

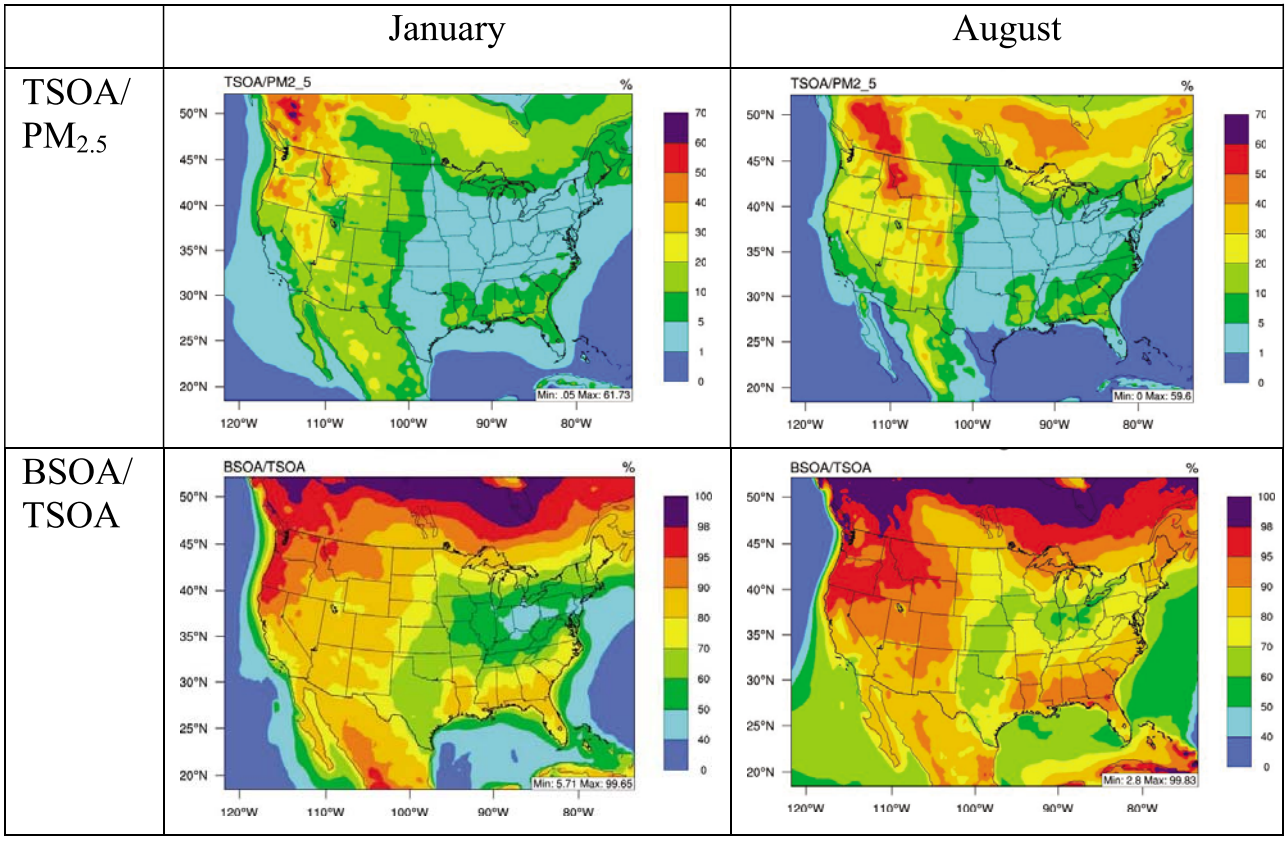

Figure 12. Simulated spatial distributions of TSOA/$PM_{2.5}$ (percent), ASOA/TSOA (percent), and BSOA/TSOA (percent) in January and August 2001.

FL) in August, implying NH_4NO_3 formation over those areas. However, NO_3^- can also be formed when DSN < 2 under cold T conditions due to a strong thermodynamic affinity between NH_4^+ and NO_3^- [*Chu*, 2004; *Mathur and Dennis*, 2003; *Pinder et al.*, 2008] (e.g., the eastern U.S. in January) or under summer conditions due to the lack of sufficient SO_4^{2-} to neutralize excess NH_3 (e.g., the western U.S. in August) (see Figure 10), although the DSN values are mostly in the range of 1.5–2. A transition value of 1.5 for DSN is therefore more appropriate than a value of 2 to indicate the formation of NH_4NO_3. Values of GR > 1, 0–1, and <0 indicate NH_3-rich, neutral, and poor conditions, respectively. NH_3-rich condition occurs in much larger areas in August than in January due to high NH_3 emissions, whereas NH_3-poor condition occurs only in a few areas in a few states (e.g., NV, AZ, NM, WY, LA, MS, WV in January and LA, MS, AL, GA, WV, VA, KY, TN, and NC in August). The full neutralization assumed in GR deviation may underestimate the amount of free NH_3 and thus NH_4NO_3, particularly under winter condition where such an assumption may not hold. This limitation is overcome by defining DSN and AdjGR and using it to correct GR [see *Zhang et al.*, 2009, equations (7)–(9)]. Compared with GR, all areas with GR < 1 now have AdjGR $\geq$ 1 in both months, reflecting greater potential for NH_4NO_3 formation over those areas, which is consistent with the adjusted DSN value to indicate NH_4NO_3 formation. High values of GR and AdjGR in the western U.S. in August are due to very small molar concentrations of TNO3 in the denominator. *Ansari and Pandis* [1998] studied the responses of inorganic PM to precursor concentrations under various T, RH, and chemical conditions using an advanced inorganic thermodynamic module. Based on their results, for areas with GR < 0 in January and August shown in Figure 11, PM formation is insensitive to an increase in TSO4; nonlinearly increase with an increase in TNH4; and is insensitive to an increase in TNO3. For areas with $0 \leq GR \leq 1$, PM response to an increase in TSO4 likely ranges from nonlinear enhanced increase to insensitive at $T \leq 298$ K depending on RH and TNO3; PM response to an increase in NH_3 likely ranges from insensitive to nonlinear near-constant increase depending on T, RH, and TNO3; PM response to an increase in TNO3 likely ranges from insensitive to nonlinear enhanced increase depending on T, RH, and TNH4. For areas with GR > 1, PM response to an increase in sulfate is generally nonlinear enhanced increase at $T \leq 275$ K and linear constant increase at T > 275 K; PM response to an increase in NH_3 ranges from nonlinear enhanced increase to insensitive depending on T, RH, and TNO3; PM response to an increase in TNO3 ranges from insensitive to linear reduced increase depending on T, RH, and TNH4. For areas with $GR \leq 1$ and GR > 1, NO_3^- is most sensitive to changes in NH_3 because of abundance of TNO3 and to changes in TNO3 because of abundance of free NH_3, respectively.

[24] Figure 12 shows spatial distributions of three mass ratios that provide insights into SOA formation including total SOA to $PM_{2.5}$ (TSOA/$PM_{2.5}$) and biogenic SOA to TSOA (BSOA/TSOA). Low values of TSOA/$PM_{2.5}$ and

BSOA/TSOA (typically < 20%) indicate conditions with low SOA and BSOA, respectively, whereas high values (typically > 50%) indicate conditions with dominance of SOA and BSOA, respectively. TSOA accounts for <20% of $PM_{2.5}$ in most states in both months. Medium-to-high SOA formation ($\geq$20%) only occurs in a few states (i.e., OR, WA, ID, MT, and NV) in CONUS in January and in many western states (i.e., WA, MT, OR, ID, WY, CA, NV, UT, CO, AZ, and NM) in CONUS in August but in southern Canada in both months. BSOA accounts for more than 50% of TSOA in both months in most of the U.S. except for a few areas in OH, IN, PA, and KY in January, indicating a dominance of BSOA in TSOA. ASOA, as the difference between TSOA and BSOA, accounts for more than 20% of TSOA in the coastal area in CA, central plains, and many states in the eastern U.S. in both months.

5. Sensitivity Studies

[25] A number of sensitivity simulations are conducted to evaluate the responses of O_3 and $PM_{2.5}$ to changes in emissions, T, and treatments of isoprene SOA and cloud processes, which in turn affect their exports out of PBL and into global troposphere. Figure 13 shows absolute changes in monthly mean hourly O_3 and $PM_{2.5}$ concentrations from sensitivity simulations C1–C4 and C6. Without isoprene emissions, C1 predicts lower O_3 over areas with high isoprene emissions in the baseline simulation, particularly in August over CA and the eastern U.S. where O_3 decreases up to 4 ppb ($\sim$10%) due to lower concentrations of O_3 precursors such as isoprene, HCHO, high molecular weight aldehydes (ALD2), CO, and HO_2. O_3 increases slightly over other areas because the effect of increased NO_2 (thus increased photolytic rates of NO_2) dominates over that of decreased isoprene and other O_3 precursors. $PM_{2.5}$ concentrations simulated from C1 decrease up to 4 μg m^{-3} ($\sim$16%) in January but increase slightly (up to 1.6 μg m^{-3} or $\sim$13%) over most of the domain in August. Since CMAQ v4.4 used in this study does not include SOA formation from isoprene photo-oxidation, removing isoprene emissions can only affect $PM_{2.5}$ indirectly via $PM_{2.5}$ gaseous precursors in C1. SOA formation, however, increases slightly in January due to an enhanced oxidation of VOC precursors by additional OH radicals available for such oxidations (which would otherwise be consumed by isoprene and its byproducts), although the total level of the OH radicals is reduced in C1 as compared with the baseline simulation. The decrease in $PM_{2.5}$ in January is primarily due to the decrease in NH_4NO_3, which may be attributed to several reasons. For example, the gas-aerosol thermodynamic equilibrium may be perturbed when isoprene emissions are excluded, which favors the partitioning of total nitrate into the gas phase (i.e., increased HNO_3 and decreased NO_3^-). Such a perturbation may have been initiated by the small increase in the concentrations of absorbing organic mass (due to increases in SOA), which shifts the gas-aerosol equilibrium toward the aerosol phase, thus decreasing gas-phase concentration of SOA precursors. As a result, NO_2 may be oxidized by more OH radicals (which otherwise would be consumed by VOCs) to form more HNO_3 (despite reduced total levels of OH radical). Decreased NO_2 gives lower N_2O_5 concentrations, leading to lower NH_4NO_3. Concentrations of SO_4^{2-} also decrease slightly due to reduced gas-phase oxidation of SO_2 by slightly reduced OH radical and reduced aqueous-phase oxidation by H_2O_2 as a result of lower HO_2 concentrations (and thus lower H_2O_2 production). Removing terpene emissions in C2 also reduces O_3 over areas with large terpene emissions in January but it increases O_3 by up to 1.6 ppb ($\sim$3%) over most of the domain in August, which is different from that of removing isoprene emissions. Lower O_3 over the western and southeastern U.S. in January is due to lower O_3 precursors such as NO_2, CO, ethane (ETH) in the eastern U.S., and HCHO in the western U.S. Higher O_3 in August is due to increased HCHO and HO_2 over the western U.S. and increased NO_2 over the whole domain. These perturbations are caused by changes in the total absorbing organic mass (due to reductions in SOA when terpene emissions are removed), which alters the gas-aerosol partitioning and subsequently affects the entire gas-phase chemical system.

[26] Similar to C1, C2 reduces $PM_{2.5}$ in January by up to 4 μg m^{-3} (or up to $\sim$60%). C2 also reduces $PM_{2.5}$ in August by up to 7 μg m^{-3} (or up to $\sim$80%), which is different from C1. Since terpene is an important precursor to SOA, the removal of its emissions leads to a substantial reduction of BSOA from terpene oxidation that dominates changes in $PM_{2.5}$ in both months. Reduction in BSOA results in a lower absorbing organic mass, which shifts the gas-aerosol equilibrium toward the gas phase, thus decreasing ASOA in both months. Removing terpene emissions also results in reduced NH_4NO_3 in January for the same reason given previously. The simulated impact of terpenes on SOA (thus $PM_{2.5}$), however, represents an upper limit. It depends strongly on the enthalpy of vaporization, which has a value of 156 KJ mol^{-1} in CMAQ v4.4. This value has been reduced to 40 KJ mol^{-1} in CMAQ v4.7, which would also reduce the impact of terpenes on $PM_{2.5}$.

[27] In C3 and C4, the emissions of five LMW AVOCs with the carbon number <8 (i.e., HCHO, ALD2, PAR, OLE, and ETH) and those of two HMW AVOCs with the carbon number > 8 (i.e., TOL and XYL) are removed respectively to study their different roles in O_3 and $PM_{2.5}$ formation. As expected, removing emissions of LMW AVOCs reduces O_3 by up to 2.4 ppb ($\sim$8%) in January and 5 ppb ($\sim$10%) in August because of reduced O_3 precursors including LMW anthropogenic VOCs, CO, and HO_2. $PM_{2.5}$ simulated from C3 also decreases up to 4 μg m^{-3} ($\sim$16%) in January but increases slightly (up to 0.8 μg m^{-3} or $\sim$8%) over most of the domain in August for the similar reasons as C1. Removal of emissions of HMW AVOCs in C4 increases O_3 in a similar way to C2 in August. It decreases O_3 throughout the domain in January because of reduced O_3 precursors such as HCHO, ALD2, CO, HO_2, although NO_2 mixing ratios increase throughout the domain (which is different from the reduction seen in NO_2 in C2). TOL and XYL are major contributors to ASOA formation. As expected, removal of their emissions reduces $PM_{2.5}$ throughout the domain up to 4 μg m^{-3} ($\sim$16%) in January and up to 0.8 μg m^{-3} ($\sim$8%) in August. The smaller decrease in $PM_{2.5}$ as compared with C2 is due to the smaller contribution of ASOA to $PM_{2.5}$ than BSOA.

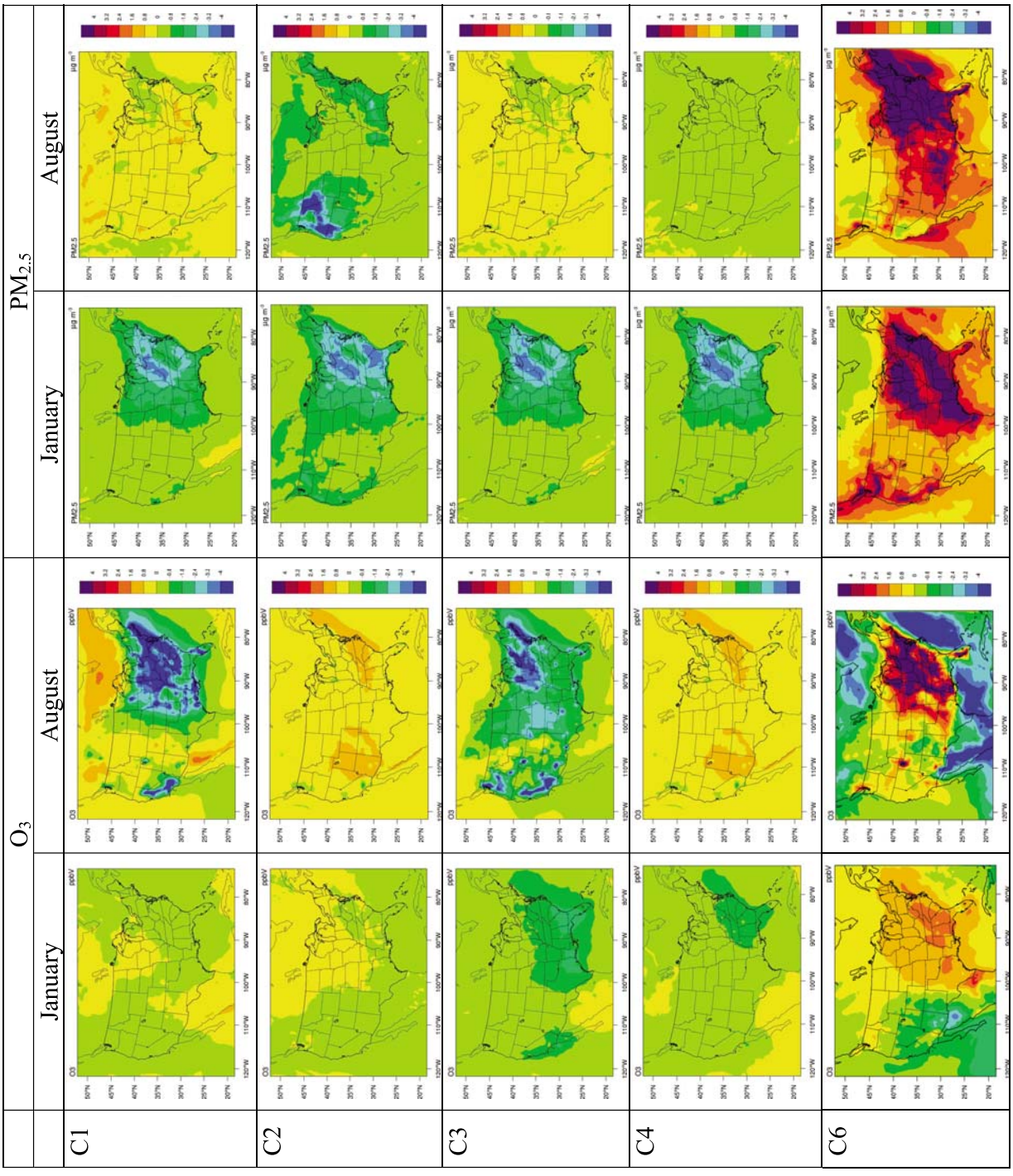

Figure 13. Absolute differences between monthly mean O_3 mixing ratios (in ppb) and $PM_{2.5}$ concentrations ($\mu g\ m^{-3}$) between sensitivity simulations C1–C4 and C6 and baseline simulations in January and August 2001.

[28] C5 is conducted to quantify the contributions of isoprene SOA to TSOA and $PM_{2.5}$. As shown in Figure 14, BSOA simulated in C5 increases by up to 0.4 (288.8%) and 1.1 $\mu g\ m^{-3}$ (729.4%) in January and August, respectively. Interestingly, $PM_{2.5}$ decreases by up to 3.5 $\mu g\ m^{-3}$ (−19.6%) in January, due to decreases in the concentrations of NH_4^+, SO_4^{2-}, and NO_3^-. Isoprene-induced SOA increases the mass concentrations of the absorbing organic matter, which alters the gas-aerosol equilibrium. For regions with high biogenic SOA (e.g., eastern U.S.), the perturbation due to changes in the gas-aerosol equilibrium accumulates over time steps and leads to increased isoprene, which consumes more NO_3 radicals, leading to lower N_2O_5 level, thus lowering particulate nitrate and ammonium concentrations. For regions with high SO_2 emissions, the perturbation leads to lower OH concentrations, which leads to lower concentrations of SO_4^{2-} and NH_4^+. $PM_{2.5}$ increases by up to 1.1 $\mu g\ m^{-3}$ (46.4%) in August, because the increase in BSOA dominates over the decreases in secondary inorganic $PM_{2.5}$.

[29] As shown in the aforementioned process analysis, the roles of cloud processes are intricate, and may either increase or decrease species concentrations, depending on the dominance of the subprocesses associated with clouds. Turning off cloud processes including convective mixing, cloud attenuation of clear-sky photolytic rates, aqueous-phase chemistry, cloud scavenging and wet deposition (i.e., C6, see Figure 13) causes up to 2.8 ppb (up to 38%, mostly within 4–16%) increase in O_3 mixing ratio over the central and eastern U.S. and up to 3.6 ppb (up to −9%, mostly within −4%) decrease in the western U.S. in January and up to 9.2 ppb (up to 23%, mostly within 2–16%) increases over most of the domain in August. These changes result from changes in O_3 and O_3 precursors without simulating cloud processes. In the absence of clouds, stronger shortwave radiation causes stronger photolysis; mixing ratios of NO_2 and VOCs are also higher due to lack of cloud scavenging. These changes, in particular, enhanced photolysis, are found to increase O_3 mixing ratios in most of the domain. On the other hand, higher NO decreases O_3 through NO titration and reduced vertical mixing may inhibit downward transport of high O_3 from free troposphere to the PBL and surface, leading to a reduction of O_3 mixing ratios in some areas in the western U.S. While *Walcek et al.* [1997] and *Zhang et al.* [1998] reported decreased O_3 formation rates by 30–90% and 16–43%, respectively, under summer urban/rural cloudy conditions due to aqueous-phase radical reactions involving dissolved HO_2 and hydroperoxy ion (O_2^-) simulated in a box model. On the other hand, *Liang and Jacob* [1997] found that the maximum O_3 depletion due to cloud chemistry in the tropics and midlatitudes summer is less than 3% based on a 3-D atmospheric model. These in-cloud reactions, however, are not included in the aqueous-phase chemistry used in CMAQ thus cannot explain lower O_3 mixing ratios in the presence of clouds. $PM_{2.5}$ concentrations without cloud processes increase throughout nearly the entire domain in both months by up to 8.6 $\mu g\ m^{-3}$ (up to 268%, mostly within 20–80%) in January and up to 19 $\mu g\ m^{-3}$ (up to 311%, mostly within 20–100%) in August, due to the enhanced reaction rates of $PM_{2.5}$ gaseous precursors to form HNO_3, H_2SO_4, and SOA precursors and the omission of the cloud scavenging and wet deposition that dominate over the aqueous-phase production of SO_4^{2-}.

[30] Figure 15 shows the absolute differences in simulated O_3 and $PM_{2.5}$ concentrations by future-year sensitivity simulations F1−F4. As summarized in Table 4, F4 is based on projected emissions for 2020 by IPCC SRES A1B scenario, with significant increases (44–57%) in the total global emissions of NO_x, VOCs, and SO_2 and moderate increases (15–18%) in those of CO, BC and OC [*IPCC*, 2001]. O_3 mixing ratios in January decrease in CA and the eastern U.S. where O_3 formation is VOC-limited. While increases in VOCs and CO emissions lead to increased in O_3, increases in NO_x emissions lead to decreased O_3 due to titration; the latter effect dominates, resulting in a net decrease in O_3 mixing ratios. For remaining areas in the western U.S., the effect of increased VOCs emissions dominates, resulting in a net increase in O_3 formation. O_3 formation in August is NO_x-limited over most of the domain except for several major metropolitan areas such as LAX, San Francisco, CHI, and NYC (see Figures 7–9 and Table 7). O_3 mixing ratios in August increase throughout the domain due mainly to increased VOCs in those metropolitan areas where O_3 formation is VOC-limited and mainly to increased NO_x and CO for the remaining areas where O_3 formation is NO_x-limited. $PM_{2.5}$ concentrations increase in the western U.S. but decrease in the eastern U.S. in January. While the concentrations of BC, primary OC, and SOA increase throughout the domain due to increased emissions of BC, primary OC, and VOCs, NH_4^+ and NO_3^- concentrations decrease over nearly the entire domain due to perturbed thermodynamic equilibrium that favors the presence of total nitrate as HNO_3 in the gas phase as well as increased SO_4^{2-} concentrations that force some NO_3^- back to the gas phase over most of the domain except for a few states in the Middle West. The competition between the two leads to a net increase in the western U.S., and a net decrease in the central plains and eastern U.S. $PM_{2.5}$ concentrations increase up to 7 $\mu g\ m^{-3}$ (∼60%) throughout the domain in August, due to increases in NH_4^+, NO_3^-, SO_4^{2-}, and SOA.

[31] Scenario F2 is based on the IPCC SRES B1 scenario which features moderate increases in the total global emissions of NO_x (by 24.69%) and SO_2 (by 8.12%) but small-to-moderate decreases in those of CO (by −14.37%), VOCs (by −0.71%), BC (by −12.1%), and OC (by −12.16%) [*IPCC*, 2001]. Similar to F1, increases in NO_x emissions in F2 lead to decreased O_3 in January, despite to a lesser extent, due to smaller increases in NO_x emissions. In addition, decreased CO and VOCs also lead to decreased O_3. In August, O_3 increases due to increased NO_x emissions over all areas except for several major metropolitan areas where O_3 formation is VOC-limited and decreased O_3 occurs in response primarily to increased NO_x and to a much lesser extent to decreased VOCs. $PM_{2.5}$ decreases throughout the domain in January, because of decreases in BC, primary OC, NH_4^+, NO_3^-, and SOA throughout the domain and decreases in SO_4^{2-} in the eastern U.S. The decreases in secondary PM are due to decreases in OH, HO_2, and organic radicals as well as the perturbations in aerosol thermodynamic equilibrium that favors HNO_3 as a dominant species for total nitrate. In August, $PM_{2.5}$ increases over most of the domain except for several states

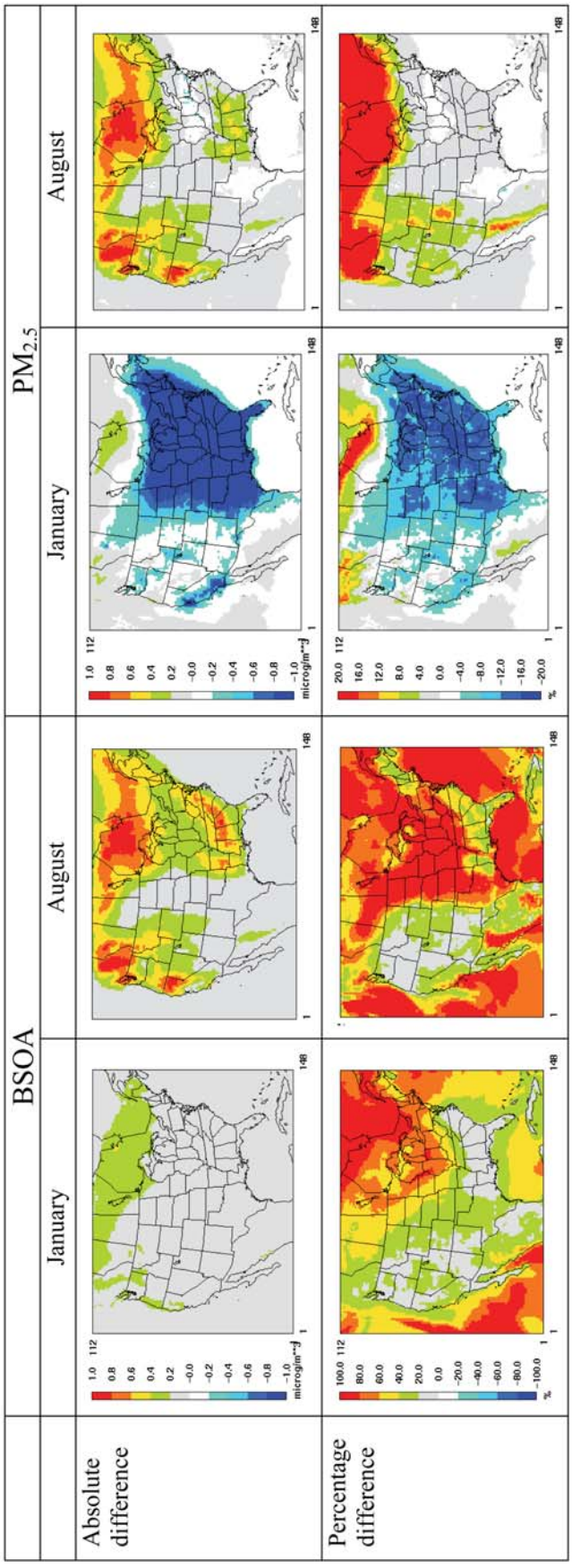

Figure 14. Absolute and percentage differences between monthly mean BSOA and $PM_{2.5}$ concentrations ($\mu g\ m^{-3}$) between sensitivity simulation C6 and baseline simulations in January and August 2001.

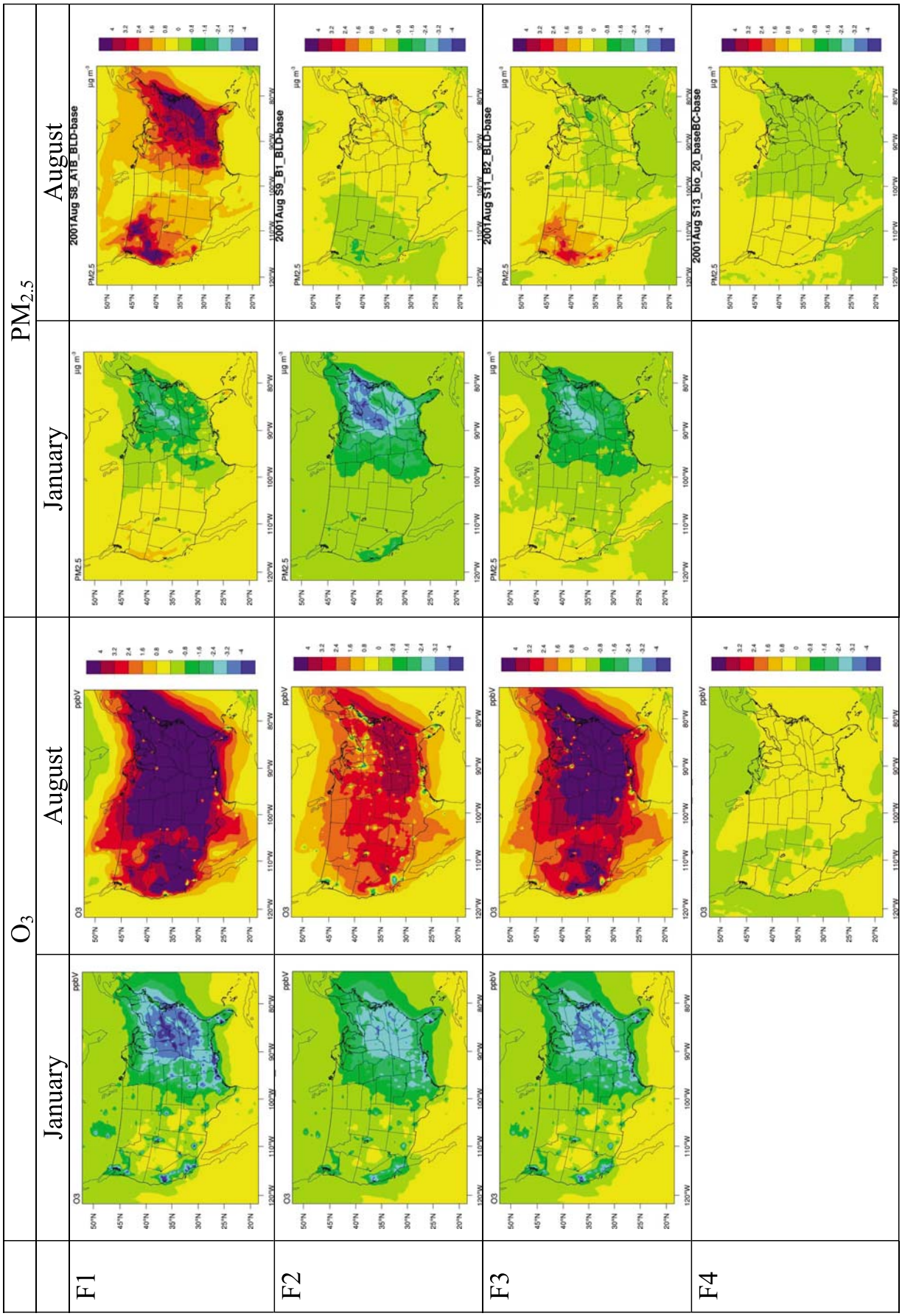

Figure 15. Absolute differences between monthly mean O_3 mixing ratios (in ppb) and $PM_{2.5}$ concentrations ($\mu g\ m^{-3}$) between sensitivity simulations F1–F4 and baseline simulations in January and August 2001.

in the western U.S., resulting from increased NH_4^+, NO_3^-, and SO_4^{2-} but decreased BC, primary OC, and SOA over most of the domain.

[32] Scenario F3 is based on the IPCC SRES B2 scenario, with moderate increases (13.71−33.44%) in the total global emissions of NO_x, CO, VOCs, BC, and OC and but moderate decreases in those of SO_2 (by −11.16%) [*IPCC*, 2001]. Responses of O_3 in both months and $PM_{2.5}$ in January are overall similar to F1, although to a lesser extent due to smaller increases in NO_x, VOCs, BC, and OC. While $PM_{2.5}$ also increases over the western U.S., it decreases (instead of increase as simulated by F1) over some areas in the eastern U.S., due to the dominance of decreased SO_4^{2-} and NH_4^+ as a result of decreased SO_2 and decreased OH.

[33] Scenario F4 uses the same emissions as the baseline simulation but with increased BVOCs emissions (e.g., isoprene, terpene, CO, NO, HCHO, and ALD2), in response to an increased PBL T of 0.71°C, which is the largest T change predicted by IPCC for 2020 among all SRES future scenarios [*IPCC*, 2001]. Increased PBL T by 0.71°C enhances the emissions of isoprene and terpene by 8.0% and 7.7%, respectively, NO by 3%, and CO, HCHO, and ALD2 by 6.5%. Their concentrations increase by 0.4 ppb (<8%) for ALD2, 4 ppb (<2%) for CO, 1 ppb (<10%) for HCHO, 1ppb (<15%) for isoprene, 0.16 ppb (<15%) for terpene. In response to these changes, O_3 increases up to 0.8 ppb in the LAX basin, CHI, Detroit, Atlanta, and New England area. Over most of the domain, average surface O_3 increases by less than 0.5 ppb. *Aw and Kleeman* [2003] conducted a 3-D Eulerian modeling of the impact of T variability on O_3 and PM in the South Coast (Los Angeles) Air basin for the period September 23−25, 1996. They found that peak simulated O_3 concentrations increased by 7 ppb for the +2 K increase in T, which is greater than the increase in this study; this is because the T increase used here is smaller than that of *Aw and Kleeman* [2003]; also, the value of 0.8 ppb is on a monthly mean basis.

6. Conclusions

[34] A full-year detailed process analyses using the PA tool and additional analyses of indicators for the sensitivity of O_3 and $PM_{2.5}$ to their precursors are conducted to gain an in-depth understanding of the processes controlling the fate of air pollutants on urban/regional scales, their potential impact on global air quality and climate, and implications to emission control policies. A total of nineteen 1 month sensitivity simulations are conducted to study the effect of speciated VOC emissions and IPCC projected emission scenarios on simulated O_3 and $PM_{2.5}$. For the formation and fate of O_3 and O_x, the most influential processes are vertical transport, gas-phase chemistry, and cloud processes for their production, and dry deposition and horizontal transport for their removal; the contribution of PM processes is small. For $PM_{2.5}$, primary PM emissions and PM processes are the two major contributors to its production, and cloud processes and horizontal/vertical transport contribute the most to its removal; contributions of dry deposition are relatively small. The export of O_3 and O_x from the U.S. PBL to free troposphere occurs primarily in summer and at a rate of 0.16 and 0.65 Gmoles day^{-1}, respectively. In contrast, the export of $PM_{2.5}$ occurs in all seasons and at rates of 25.68−34.18 Ggrams day^{-1}, indicating a need to use different control strategies for O_3 and $PM_{2.5}$, e.g., monitor and control $PM_{2.5}$ throughout the year, rather than just for high O_3 seasons (May−September). The exports of O_3 and $PM_{2.5}$ affect both air quality and climate in the global environment. For example, while the exports of O_3 in summer and BC, absorbing OM, and NH_4^+ in all seasons can potentially enhance warming, those of other PM species help cool the atmosphere.

[35] Based on the simulated spatial distributions of P_{H2O2}/P_{HNO3}, VOC-limited O_3 chemistry dominates in most areas except for some areas in the western and northeastern U.S. in winter. Some states in the central plains experience a transition from VOC-limited to NO_x-limited conditions in March. While major cities remain VOC-limited throughout the remaining months, all other areas are NO_x-limited with the largest NO_x-limited extent in July. Among 16 representative sites examined, VOC-limited chemistry dominates at 12 urban, suburban, and rural sites in January and NO_x-limited chemistry dominates at 8 urban, rural, and national park sites in August. These results suggest effective strategies that include nationwide NO_x emission control, integrated control of NO_x and VOCs emissions for large cities during high O_3 seasons (May−September), and consideration of monthly variation of O_3 sensitivity for specific regions. With the established transition values for NO_x- and VOC-limited O_3 chemistry in the literature, P_{H2O2}/P_{HNO3}, $HCHO/NO_y$, and $HCHO/NO_z$ provide the most robust photochemical indicators for O_3 sensitivity in both winter and summer, $H_2O_2/(O_3 + NO_2)$ is robust in winter and NO_y is robust in summer. The transition values for $H_2O_2/(O_3 + NO_2)$ in summer and those for other indicators such as H_2O_2/HNO_3, NO_y, O_3/NO_x, O_3/NO_y, and O_3/NO_z in both summer and winter need to be adjusted to provide a more consistent result with the robust indicators.

[36] Secondary inorganic PM is dictated by the abundance of TNH3, TSO4, and TNO3 via a complex partitioning process between the gas and the aqueous phase. NH_3-rich condition occurs in much larger areas in August than in January due to high NH_3 emissions, whereas NH_3-poor condition occurs only in a few areas in a few states in January and August. Nitrate can be formed when sulfate neutralization is insufficient with DSN values of 1.5−2 under cold temperature conditions due to a strong thermodynamic affinity between NH_4^+ and NO_3^- (e.g., in the eastern U.S. in January) and under summer conditions in an NH_3-rich environment due to a lack of sufficient SO_4^{2-} to neutralize NH_4^+ (e.g., in the western U.S. in August). Compared with the GR that assumes a full sulfate neutralization and thus underestimates the amount of NH_4NO_3 formed, AdjGR that is based on DSN is superior and works well under conditions with insufficient sulfate neutralization. Depending on the GR values and ambient conditions such as T and RH, PM formation may be sensitive or insensitive to an increase in TNH3, TSO4, or TNO3 (thus the emissions of NH_3, SO_2, and NO_x). PM nitrate is most sensitive to changes in NH_3 because of abundance of TNO3 in areas with GR $\leq$ 1 (e.g., some areas in the western U.S. in January) and to changes in TNO3 because of abundance of free NH_3 in areas with GR > 1 (e.g., the western U.S. in August). Secondary organic PM formation is controlled by the relative abundance of AVOCs and BVOCs. Medium-to-

high SOA formation (>20%) only occurs in a few states in January and in many western states in August. BSOA dominates SOA, accounting for more than 50% of TSOA in both months in most of the U.S.

[37] Isoprene emissions increase O_3 by up to 4 ppb (~10%) due to higher O_3 precursors particularly in August over CA and the eastern U.S and $PM_{2.5}$ by up to 4 $\mu g\ m^{-3}$ (~16%) in January but decrease $PM_{2.5}$ slightly (up to 1.6 $\mu g\ m^{-3}$ or ~13%) over most areas in August, because of decreased NO_3^- and SO_4^{2-}. They also increase SOA by up to 0.4 (288.8%) and 1.1 $\mu g\ m^{-3}$ (729.4%) in January and August, respectively. Terpene emissions increase simulated O_3 over areas with large terpene emissions in January but decrease O_3 by up to 1.6 ppb (~3%) over most areas in August. Higher O_3 over western and southeastern U.S. in January in the baseline simulation with isoprene emissions is due to higher O_3 precursors such as NO_2, CO, ETH, and HCHO. Lower O_3 in August is due to decreased HCHO and HO_2 over the western U.S. and decreased NO_2 over the whole domain. As an important precursor to SOA, the emissions of terpene increase $PM_{2.5}$ in January by up to 4 $\mu g\ m^{-3}$ (~60%) and in August by up to 7 $\mu g\ m^{-3}$ (~80%). Emissions of LMW AVOCs increase O_3 by up to 2.4 ppb (~8%) in January and 5 ppb (~10%) in August because of increased O_3 precursors including LMW AVOCs, CO, and HO_2. They also increase $PM_{2.5}$ by up to 4 $\mu g\ m^{-3}$ (~16%) in January but decrease them slightly (up to 0.8 $\mu g\ m^{-3}$ or ~8%) over most areas in August. The emissions of HMW AVOCs in C4 increase O_3 throughout the domain in January because of increased O_3 precursors such as HCHO, ALD2, CO, HO_2, although NO_2 mixing ratios decrease throughout the domain. TOL and XYL are major contributors to ASOA formation. Their emissions increase $PM_{2.5}$ throughout the domain up to 4 $\mu g\ m^{-3}$ (~16%) in January and up to 0.8 $\mu g\ m^{-3}$ (~8%) in August. Overall, among the four types of VOC emissions examined, isoprene and LMW AVOCs are more important than HMW AVOCs and terpenes in O_3 formation, and terpenes and isoprene contribute more to SOA and $PM_{2.5}$ than LMW and HMW AVOCs.

[38] Cloud processes may either increase or decrease species concentrations, depending on the dominance of the subprocesses associated with clouds. These processes can cause up to 2.8 ppb (up to 38%) increase in O_3 mixing ratio over the central and eastern U.S. and up to 3.6 ppb (up to −9%) decrease in the western U.S. in January and up to 9.2 ppb (up to 23%) increases over most of the domain in August. $PM_{2.5}$ concentrations decrease throughout nearly the entire domain in both months by up to 8.6 $\mu g\ m^{-3}$ (up to 268%) in January and up to 19 $\mu g\ m^{-3}$ (up to 311%) in August. While the increases in O_3 and $PM_{2.5}$ in the absence of clouds are caused by the enhanced photolysis and oxidation reaction rates of their gaseous precursors and the omission of the cloud scavenging and wet deposition that dominate over the aqueous-phase production of SO_4^{2-}, the decreases are attributed to increased NO titration and reduced vertical mixing.

[39] Under all future emission scenarios, surface O_3 mixing ratios may increase in summer, surface $PM_{2.5}$ concentrations may increase or decrease, depending on the emission scenarios and the geographical regions. Under future climate conditions with 0.71°C increase in surface temperatures, surface O_3 mixing ratios may increase in summer and surface $PM_{2.5}$ concentrations may decrease in the eastern U.S. but increase in the western U.S.

[40] **Acknowledgments.** This work was performed under the National Aeronautics and Space Administration Award NNG04GJ90G. The authors thank J.-P. Huang, a former postdoctoral researcher at NCSU, for postprocessing some CMAQ results during the early stage of this work, and X.-M. Hu, a former graduate student at NCSU, for postprocessing some CMAQ results.

References

Andreani-Aksoyoglu, S., C.-H. Lub, J. Kellera, A. S. H. Prévót, and J. S. Chang (2001), Variability of indicator values for ozone production sensitivity: A model study in Switzerland and San Joaquin Valley (California), *Atmos. Environ.*, *35*, 5593–5604, doi:10.1016/S1352-2310(01)00278-3.

Ansari, A. S., and S. N. Pandis (1998), Response of inorganic PM to precursor concentrations, *Environ. Sci. Technol.*, *32*, 2706–2714, doi:10.1021/es971130j.

Aw, J., and M. J. Kleeman (2003), Evaluating the first-order effect of intraannual temperature variability on urban air pollution, *J. Geophys. Res.*, *108*(D12), 4365, doi:10.1029/2002JD002688.

Byun, D., and K. L. Schere (2006), Review of the governing equations, computational algorithms, and other components of the Models-3 Community Multiscale Air Quality (CMAQ) modeling system, *Appl. Mech. Rev.*, *59*, 51–77, doi:10.1115/1.2128636.

Chameides, W. L., R. W. Lindsay, J. L. Richardson, and C. S. Kiang (1988), The role of biogenic hydrocarbons in urban photochemical smog: Atlanta as a case study, *Science*, *241*, 1473–1475, doi:10.1126/science.3420404.

Chameides, W. L., R. D. Saylor, and E. B. Cowling (1997), Ozone pollution in the rural U. S. and the new NAAQS, *Science*, *276*, 916, doi:10.1126/science.276.5314.916.

Chu, S. H. (2004), $PM_{2.5}$ episodes as observed in the speciation trends network, *Atmos. Environ.*, *38*, 5237–5246, doi:10.1016/j.atmosenv.2004.01.055.

Dunker, A. M. (1984), The decoupled direct method for calculating sensitivity coefficients in chemical kinetics, *J. Chem. Phys.*, *81*, 2385, doi:10.1063/1.447938.

ENVIRON (2004), User's guide on Comprehensive Air Quality Model with Extensions (CAMx), version 4.10S, report, ENVIRON, Novato, Calif.

Feichter, J., and E. Roeckner (2004), Nonlinear aspects of the climate response to greenhouse gas and aerosol forcing, *J. Clim.*, *17*, 2384–2398, doi:10.1175/1520-0442(2004)017<2384:NAOTCR>2.0.CO;2.

Hammer, M.-U., B. Vogel, and H. Vogel (2002), Findings on H_2O_2/HNO_3 as an indicator of ozone sensitivity in Baden-Württemberg, Berlin-Brandenburg, and the Po valley based on numerical simulations, *J. Geophys. Res.*, *107*(D22), 8190, doi:10.1029/2000JD000211.

Heald, C. L., et al. (2008), Predicted change in global secondary organic aerosol concentrations in response to future climate, emissions, and land use change, *J. Geophys. Res.*, *113*, D05211, doi:10.1029/2007JD009092.

Hogrefe, C., B. Lynn, K. Civerolo, J.-Y. Ku, J. Rosenthal, C. Rosenzweig, R. Goldberg, S. Gaffin, K. Knowlton, and P. L. Kinney (2004), Simulating changes in regional air quality over the eastern United States due to changes in global and regional climate and emissions, *J. Geophys. Res.*, *109*, D22301, doi:10.1029/2004JD004690.

Horowitz, L. W., J. Liang, G. M. Gardner, and D. J. Jacob (1998), Export of reactive nitrogen from North America during summertime: Sensitivity to hydrocarbon chemistry, *J. Geophys. Res.*, *103*, 13,451–13,476, doi:10.1029/97JD03142.

Intergovernmental Panel on Climate Change (IPCC) (2001), *Climate Change 2001: The Scientific Basis—Contribution of Working Group I to the Third Assessment Report of the Intergovernmental Panel on Climate Change*, 881 pp., Cambridge Univ. Press, New York.

Jacob, D. J., J. A. Logan, G. M. Gardner, R. M. Yevich, C. M. Spivakovsky, S. C. Wofsy, S. Sillman, and M. J. Prather (1993), Factors regulating ozone over the united State and its export to the global atmosphere, *J. Geophys. Res.*, *98*, 14,817–14,826, doi:10.1029/98JD01224.

Jacob, D. J., J. A. Logan, and P. P. Murti (1999), Effect of rising Asian emissions on surface ozone in the United States, *Geophys. Res. Lett.*, *26*, 2175–2178, doi:10.1029/1999GL900450.

Jacobson, M. Z. (2002), Control of fossil-fuel particulate black carbon and organic matter, possibly the most effective method of slowing global warming, *J. Geophys. Res.*, *107*(D19), 4410, doi:10.1029/2001JD001376.

Jacobson, M. Z. (2005), *Fundamentals of Atmospheric Modeling*, 2nd ed., 813 pp., Cambridge Univ. Press, New York.

Jacobson, M. Z. (2008), On the causal link between carbon dioxide and air pollution mortality, *Geophys. Res. Lett.*, *35*, L03809, doi:10.1029/2007GL031101.

Jacobson, M. Z., Y. J. Kaufmann, and Y. Rudich (2007), Examining feedbacks of aerosols to urban climate with a model that treats 3-D clouds with aerosol inclusions, *J. Geophys. Res.*, *112*, D24205, doi:10.1029/2007JD008922.

Jang, J.-C. C., H. E. Jeffries, and S. Tonnesen (1995), Sensitivity of ozone to model grid resolution: II. Detailed process analysis for ozone chemistry, *Atmos. Environ.*, *29*, 3101–3114, doi:10.1016/1352-2310(95)00119-J.

Jeffries, H. E., and S. Tonnesen (1994), A comparison of two photochemical reaction mechanisms using mass balance and process analysis, *Atmos. Environ.*, *28*, 2991–3003, doi:10.1016/1352-2310(94)90345-X.

Li, Q., D. J. Jacob, J. W. Munger, R. M. Yantosca, and D. D. Parrish (2004), Export of NO_y from the North American boundary layer: Reconciling aircraft observations and global model budgets, *J. Geophys. Res.*, *109*, D02313, doi:10.1029/2003JD004086.

Liang, J., and D. J. Jacob (1997), Effect of aqueous-phase cloud chemistry on tropospheric ozone, *J. Geophys. Res.*, *102*(D5), 5993–6002, doi:10.1029/96JD02957.

Liang, J., L. W. Horowitz, D. J. Jacob, Y. Wang, A. M. Fiore, J. A. Logan, G. M. Gardner, and J. W. Munger (1998), Seasonal budgets of reactive nitrogen species and ozone over the United States, and export fluxes to the global atmosphere, *J. Geophys. Res.*, *103*, 13,435–13,450, doi:10.1029/97JD03126.

Liang, J.-Y., B. Jackson, and A. Kaduwela (2006), Evaluation of the ability of indicator species ratios to determine the sensitivity of ozone to reductions in emissions of volatile organic compounds and oxides of nitrogen in northern California, *Atmos. Environ.*, *40*, 5156–5166, doi:10.1016/j.atmosenv.2006.03.060.

Lindsay, R. W., W. L. Chameides, and J. L. Richardson (1989), Ozone trends in Atlanta, Georgia: Have emission controls been effective?, *J. Air Pollut. Control Assoc.*, *39*(1), 40–43.

Lu, C.-H., and J. S. Chang (1998), On the indicator-based approach to assess ozone sensitivities and emissions features, *J. Geophys. Res.*, *103*, 3453–3462, doi:10.1029/97JD03128.

Martin, R. V., A. M. Fiore, and A. V. Donkelaar (2004), Space-based diagnosis of surface ozone sensitivity to anthropogenic emissions, *Geophys. Res. Lett.*, *31*, L06120, doi:10.1029/2004GL019416.

Mathur, R., and R. L. Dennis (2003), Seasonal and annual modeling of reduced nitrogen compounds over the eastern United States: Emissions, ambient levels, and deposition amounts, *J. Geophys. Res.*, *108*(D15), 4481, doi:10.1029/2002JD002794.

Milford, J. B., D. Gao, A. G. Russell, and G. J. McRae (1992), Use of sensitivity analysis to compare chemical mechanisms for air quality modeling, *Environ. Sci. Technol.*, *26*, 1179–1189, doi:10.1021/es50002a606.

Milford, J. B., D. F. Gao, S. Sillman, P. Blossey, and A. G. Russell (1994), Total reactive nitrogen (NO_y) as an indicator of the sensitivity of ozone to reductions in hydrocarbon and NO_x emissions, *J. Geophys. Res.*, *99*, 3533–3542.

Murazaki, K., and P. Hess (2006), How does climate change contribute to surface ozone change over the United States?, *J. Geophys. Res.*, *111*, D05301, doi:10.1029/2005JD005873.

Nguyen, K., and D. Dabdub (2002), NO_x and VOC control and its effects on the formation of aerosols, *Aerosol Sci. Technol.*, *36*, 560–572, doi:10.1080/02786820252883801.

Pierce, R. B., et al. (2007), Chemical data assimilation estimates of continental U.S. ozone and nitrogen budgets during the Intercontinental Chemical Transport Experiment–North America, *J. Geophys. Res.*, *112*, D12S21, doi:10.1029/2006JD007722.

Pinder, R. W., R. L. Dennis, and P. V. Bhave (2008), Observable indicators of the sensitivity of $PM_{2.5}$ nitrate to emission reductions: Part I. Derivation of the adjusted gas ratio and applicability at regulatory-relevant time scales, *Atmos. Environ.*, *42*(6), 1275–1286, doi:10.1016/j.atmosenv.2007.10.039.

Pun, B. K., and C. Seigneur (2001), Sensitivity of particulate matter nitrate formation to precursor emissions in the California San Joaquin Valley, *Environ. Sci. Technol.*, *35*(14), 2979–2987, doi:10.1021/es0018973.

Seigneur, C., B. Pun, and Y. Zhang (1999), Review of methods for source apportionment in three-dimensional air quality models for particulate matter, *EPRI TR-112070*, Electr. Power Res. Inst., Palo Alto, Calif.

Seinfeld, J. H., and S. N. Pandis (2006), *Atmospheric Chemistry and Physics: From Air Pollution to Climate Change*, 1203 pp., John Wiley, Hoboken, N. J.

Sillman, S. (1995), The use of NO_y, H_2O_2, and HNO_3 as indicators for ozone-NO_x-hydrocarbon sensitivity in urban locations, *J. Geophys. Res.*, *100*, 4175–4188.

Sillman, S., and D. He (2002), Some theoretical results concerning O_3-NO_x-VOC chemistry and NO_x-VOC indicators, *J. Geophys. Res.*, *107*(D22), 4659, doi:10.1029/2001JD001123.

Sillman, S., D. He, C. Cardelino, and R. E. Imhoff (1997), The use of photochemical indicators to evaluate ozone-NO_x-hydrocarbon sensitivity: Case studies from Atlanta, New York, and Los Angeles, *J. Air Waste Manage. Assoc.*, *47*, 642–652.

Stockwell, W. R. (1986), A homogeneous gas phase mechanism for use in a regional acid deposition model, *Atmos. Environ.*, *20*, 1615–1632, doi:10.1016/0004-6981(86)90251-9.

Takahama, S., A. E. Wittig, D. V. Vayenas, C. I. Davidson, and S. N. Pandis (2004), Modeling the diurnal variation of nitrate during the Pittsburgh Air Quality Study, *J. Geophys. Res.*, *109*, D16S06, doi:10.1029/2003JD004149.

Tonnesen, G. S., and R. L. Dennis (2000a), Analysis of radical propagation efficiency to assess ozone sensitivity to hydrocarbons and NO_x: 1. Local indicators of instantaneous odd oxygen production sensitivity, *J. Geophys. Res.*, *105*, 9213–9225, doi:10.1029/1999JD900371.

Tonnesen, G. S., and R. L. Dennis (2000b), Analysis of radical propagation efficiency to assess ozone sensitivity to hydrocarbons and NO_x: 2. Long-lived species as indicators of ozone concentration sensitivity, *J. Geophys. Res.*, *105*, 9227–9241, doi:10.1029/1999JD900372.

Vijayaraghavan, K., Y. Zhang, C. Seigneur, P. Karamchandani, and H. E. Snell (2009), Export of reactive nitrogen from coal-fired power plants in the USA: Estimates from a plume-in-grid modeling study, *J. Geophys. Res.*, *114*, D04308, doi:10.1029/2008JD010432.

Vogel, B., N. Riemer, H. Vogel, and F. Fiedler (1999), Findings on NO_y as an indicator for ozone sensitivity based on different numerical simulations, *J. Geophys. Res.*, *104*, 3605–3620.

Walcek, C. J., H.-H. Yang, and W. R. Stockwell (1997), The influence of aqueous-phase chemical reactions on ozone formation in polluted and non-polluted clouds, *Atmos. Environ.*, *31*, 1221–1237, doi:10.1016/S1352-2310(96)00257-9.

Wang, K., Y. Zhang, C. Jang, S. Phillips, and B. Wang (2009), Modeling intercontinental air pollution transport over the trans-Pacific region in 2001 using the Community Multiscale Air Quality modeling system, *J. Geophys. Res.*, *114*, D04307, doi:10.1029/2008JD010807.

Wu, S., L. J. Mickley, E. M. Leibensperger, D. J. Jacob, D. Rind, and D. G. Streets (2008), Effects of 2000–2050 global change on ozone air quality in the United States, *J. Geophys. Res.*, *113*, D06302, doi:10.1029/2007JD008917.

Wu, S.-Y., S. Krishnan, Y. Zhang, and V. Aneja (2008), Modeling atmospheric transport and fate of ammonia in North Carolina, Part I. Evaluation of meteorological and chemical predictions, *Atmos. Environ.*, *42*, 3419–3436, doi:10.1016/j.atmosenv.2007.04.031.

Zhang, Y., C. H. Bischof, R. C. Easter, and P.-T. Wu (1998), Sensitivity analysis of a mixed-phase chemical mechanism using automatic differentiation, *J. Geophys. Res.*, *103*(D15), 18,953–18,979, doi:10.1029/98JD01278.

Zhang, Y., K. Vijayaraghavan, and C. Seigneur (2005), Evaluation of three probing techniques in a three-dimensional air quality model, *J. Geophys. Res.*, *110*, D02305, doi:10.1029/2004JD005248.

Zhang, Y., J.-P. Huang, D. K. Henze, and J. H. Seinfeld (2007), The role of isoprene in secondary organic aerosol formation on a regional scale, *J. Geophys. Res.*, *112*, D20207, doi:10.1029/2007JD008675.

Zhang, Y., K. Vijayaraghavan, X.-Y. Wen, K. Wang, H. E. Snell, and Z. M. Jacobson (2009), Probing into regional O_3 and particulate matter pollution in the United States: 1. A 1 year CMAQ simulation and evaluation using surface and satellite data, *J. Geophys. Res.*, *114*, D22304, doi:10.1029/2009JD011898.

M. Z. Jacobson, Department of Civil and Environmental Engineering, Stanford University, Stanford, CA 94305, USA.

K. Vijayaraghavan, Atmospheric and Environmental Research, Inc., San Francisco, CA 94111, USA.

K. Wang, X.-Y. Wen, and Y. Zhang, Department of Marine, Earth and Atmospheric Sciences, North Carolina State University, 1125 Jordan Hall, Campus Box 8208, 2800 Faucette Dr., Raleigh, NC 27695, USA.